Combined Analysis: a global approach for characterization using ray scattering: structure, texture, stress, nanocrystals, phase, reflectivity, fluorescence …

D. Chateigner, L. Lutterotti

Normandie Université, Univ. Trento

Leicester, UK, 11-12th Jul. 2017

Rietveld: Acta Cryst. (1967), J. Appl. Cryst (1969)

computers, neutrons (Gaussian peaks): powders !

Lutterotti, Matthies, Wenk: Rietveld Texture Analysis, J. Appl. Phys. (1997)

classical Rietveld + QTA (WIMV)

Morales, Chateigner, Lutterotti, Ricote: Mat. Sci. For. (2002)

Rietveld of layers (QTA, QMA) + E-WIMV

ESQUI EU FP6 project (ended Jan. 2003)

Lutterotti, Chateigner, Ferrari, Ricote: Thin Sol. Films (2004)

E-WIMV + RSA + XRR + Geom. Mean: Extended Rietveld

Chateigner, Combined Analysis, Wiley-ISTE (2010)

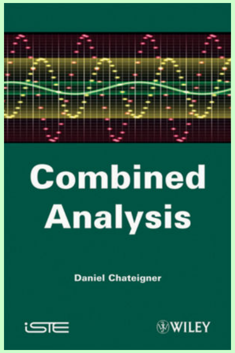

Soon in International Tables Vol H

Boullay, Lutterotti, Chateigner, Sicard: Acta Cryst A (2014)

Electron Diffraction Pattern – 2-waves Blackman correction

X-ray scattering "sees"

Texture

$f(g)_{\Phi,L}$

Structure

$|F_{\mathbf{h}}|^2_{\Phi,L}$

Real samples

Layered samples

thicknesses

roughnesses

$\rho(z)$…

Residual Stress

$\langle C_{ijkl}(g) \rangle_{\Phi,L}$

Phase

$S_{\Phi,L}$

defects (0D .. nD)

broadening

asymmetry

Rietveld: extended to lots of spectra

$$y_c(\mathbf{y}_S,\theta,\eta) = y_b(\mathbf{y}_S,\theta,\eta) + I_0 \sum_{i=1}^{N_L} \sum_{\Phi=1}^{N_\Phi} \frac{\nu_{i\Phi}}{V_{c\Phi}^2} \sum_h Lp(\theta) j_{\Phi h} |F_{\Phi h}|^2 \Omega_{\Phi h}(\mathbf{y}_S,\theta,\eta) P_{\Phi h}(\mathbf{y}_S,\theta,\eta) A_{i\Phi}(\mathbf{y}_S,\theta,\eta)$$

Texture:

$$P_h(\mathbf{y}_S) = \int_{\tilde{\varphi}} f(g,\tilde{\varphi})\, d\tilde{\varphi}$$

E-WIMV, components, Harmonics, Exp. Harmonics …

Strain-Stress:

$$\langle S \rangle_{geo}^{-1} = \left[\prod_{m=1}^{N} S_m^{\nu_m} \right]^{-1} = \prod_{m=1}^{N} S_m^{-\nu_m} = \prod_{m=1}^{N} \left(S_m^{-1} \right)^{\nu_m} = \left\langle S^{-1} \right\rangle_{geo} = \langle C \rangle_{geo}$$

Geometric mean, Voigt, Reuss, Hill …

Layering:

$$A_{i\Phi} = \frac{\nu_{i\Phi} \sin\theta_i \sin\theta_o}{\bar{\mu}_i (\sin\theta_i + \sin\theta_o)} \left\{ 1 - e^{-\bar{\mu}_i \tau_i W} \right\} \prod_{k<i} e^{-\bar{\mu}_k \tau_k W}$$

$$W = \frac{1}{\sin\theta_i} + \frac{1}{\sin\theta_o}$$

Stacks, coatings, multilayers …

Line Broadening:

Popa, Delft, Warren, Ufer: Crystallite sizes, shapes, microstrains, distributions
0D-3D defects, turbostratism

X-Ray Reflectivity (specular):

Matrix, Parrat, DWBA, EDP …

X-Ray Fluorescence/GiXRF:

De Boer

Electron Diffraction Patterns:

2-waves Blackman

Combined Analysis approach

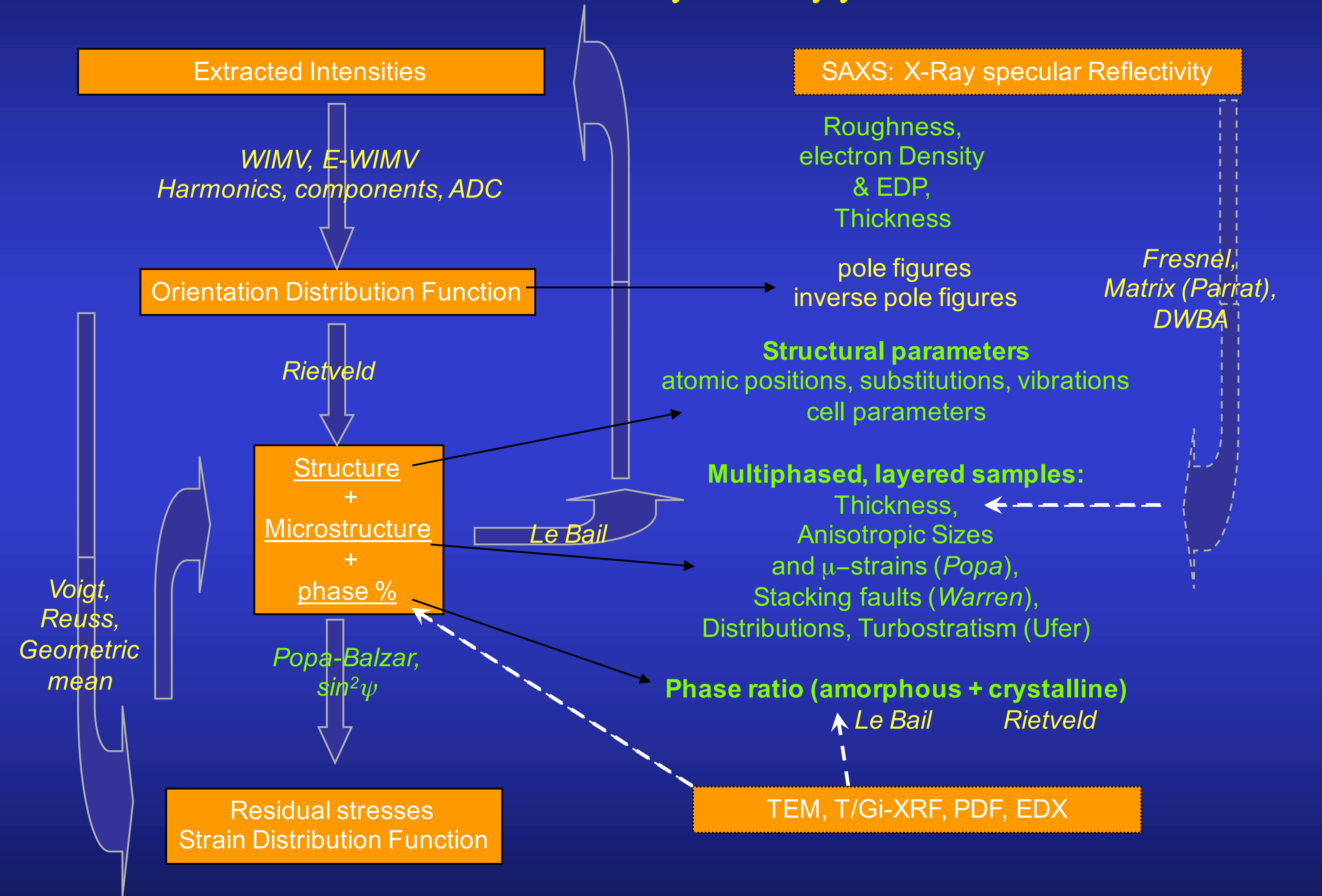

Minimum experimental requirements

1D or 2D Detector +
4-circles diffractometer
(CRISMAT – ANR EcoCorail)

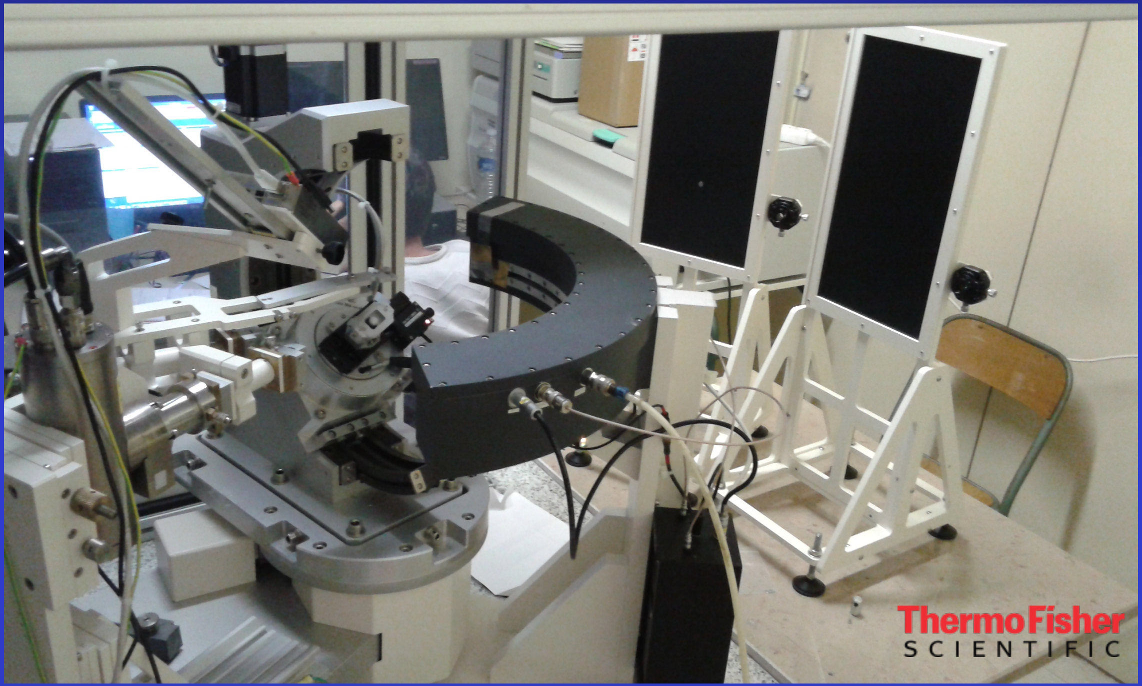

~1000 experiments (2θ diagrams)
in as many sample orientations

+

Instrument calibration
(peaks widths and shapes,
misalignments, defocusing …)

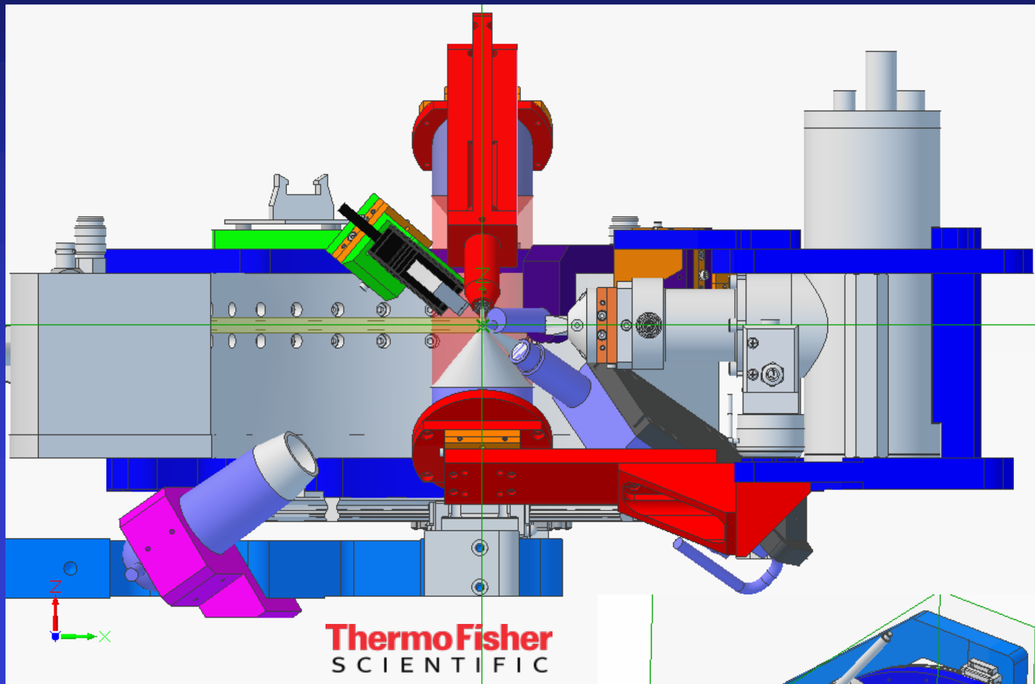

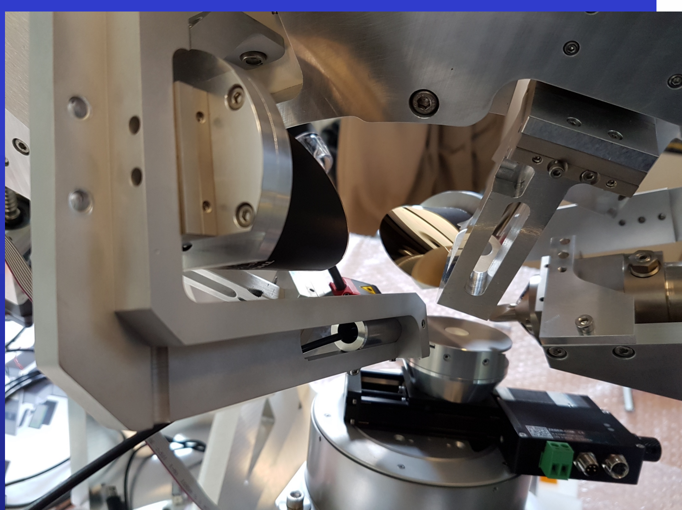

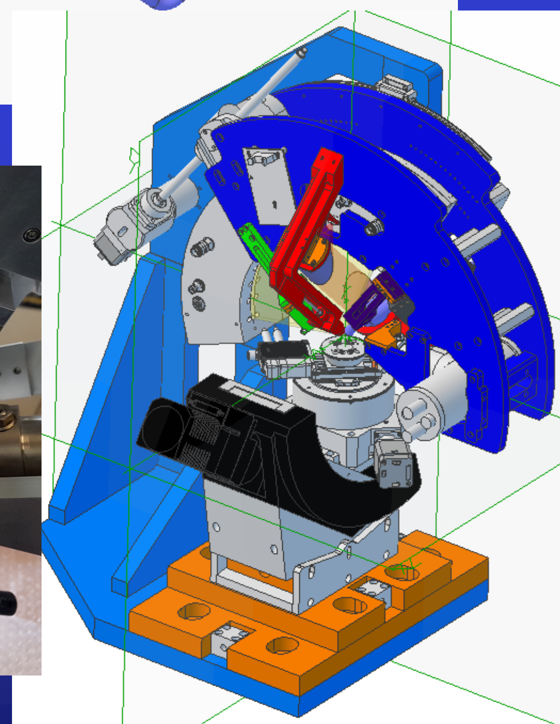

SOLSA

XRD-XRF-Raman-FTIR Combined Analysis (SOLSA EU projet)

Combined Analysis cost function

$$WSS = \sum_{t=1}^{N_p} u_t \sum_{i=0}^{N_t} w_{it} \left(y_{itc} - y_{ito} \right)^2$$

For each pattern t: w_{it} : weight, usually $1/y_i = \sigma^2$.

u_t : weight of each pattern t
should be used to adjust the importance we want to give to a particular technique or pattern with respect to the others

Independent measurements

Different wavelengths and rays

Reflectivity: thickness, roughness, electron density profiles

X-ray Fluorescence: composition

Spectroscopies: local structures (PDF, FTIR, Mossbauer …), eventually anisotropic (P-EXAFS, ESR, Raman …), Element profiles (SIMS, RBS …) …

Physical models: magnetisation, conductivity …

Environments: applied fields

XRD Calibration

ω = 20°

60°

χ

0°

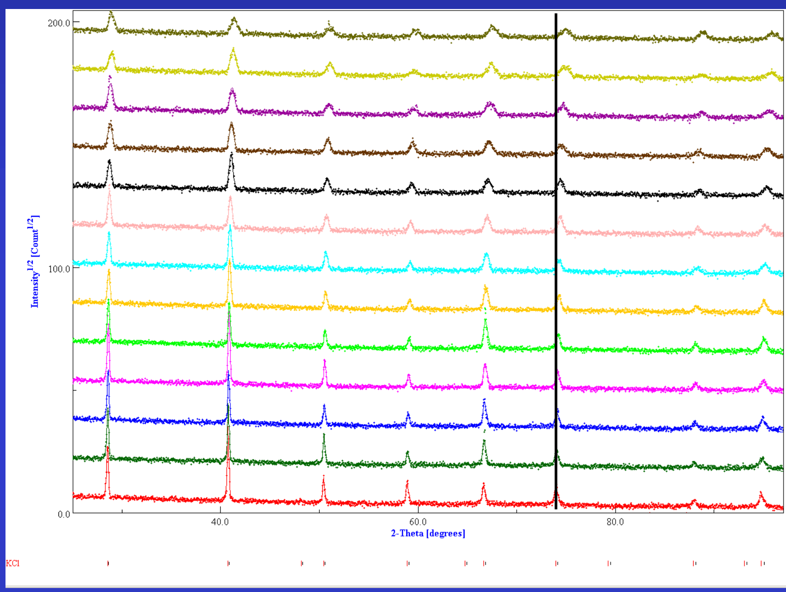

ω = 40°

60°

χ

0°

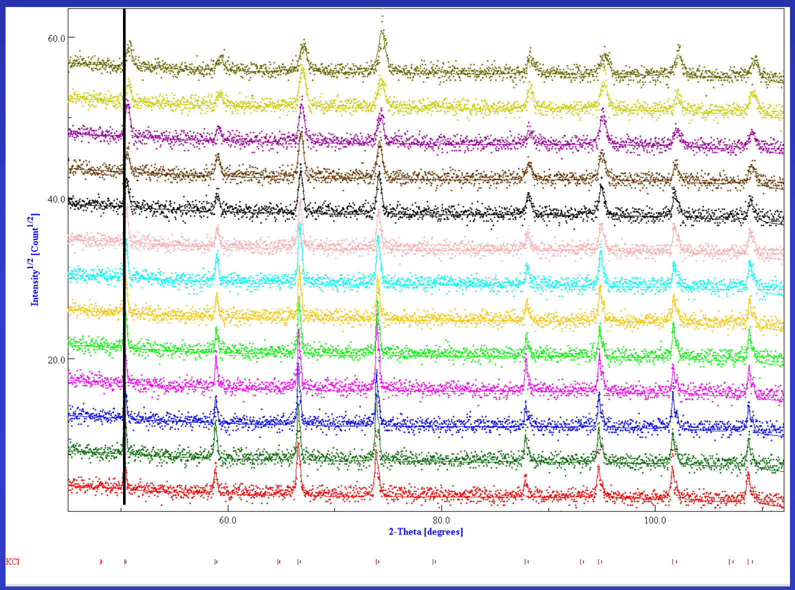

LaB_6, CeO_2, KCl, …

→

FWHM (ω, χ, φ, 2θ, η, κ …)
2θ shift
gaussianity
asymmetry
misalignments …

Minimization algorithms

- Can be fully used in the method (everywhere)

- Marquardt Least Squares (based on steepest decrease and Gauss-Newton)
  - Efficient, best with few parameters, near the solution
- Evolutionary computation (or genetic algorithm)
  - Slow, not efficient, requires a lot of resources
  - Unlimited number of parameters
  - Can start far from the solution
- Simulated annealing (the solution proceed like a random walk, but the walking step decreases as temperature decreases)
  - In between the Marquardt and evolutionary algorithms
- Simplex (generates n+1 starting solutions as vertices of a polygon, n number of parameters, and contract/expand the polygon around the minima)
  - Slow on convergence
  - Remains close to the solution, but explore more minima with respect to the Marquardt

Full-Pattern Search-Match

maud.radiographema.com   www.iutcaen.unicaen.fr

Diffraction pattern and sample composition

Upload diffraction pattern: [   ] Parcourir...

Atomic elements in the sample: O Al Ca F Zn

☐ Sample nanocrystalline

Experiment details

Radiation:
- (●) X-ray tube: Cu
- ( ) Other : x-ray Wavelength (Å): 1.540598

Instrument geometry:
- (●) Bragg-Brentano (theta-2theta)
- ( ) Bragg-Brentano (2theta only), omega: 10
- ( ) Debye-Scherrer
- ( ) Transmission

Instrument broadening function: Medium

Search and quantify

☐ Extra output (for debugging)

Structures database: CODstructures

30s later
>375000 COD structures

Found phases and quantification:

Phase ID	name	vol. (%)	wt. (%)	crystallites (Å)	microstrain
9004178	Zincite	16.8284	23.9708	2148.26	0.00028435
9009005	Fluorite	42.5522	33.9388	2117.08	0.000363147
9007498	Corundum	37.2197	37.2493	1889.82	0.000267779
2300112	zinc_oxide	3.39971	4.84114	1754.74	6.98311e-05

Final Rietveld analysis, Rw: 0.159468, GofF: 1.95869

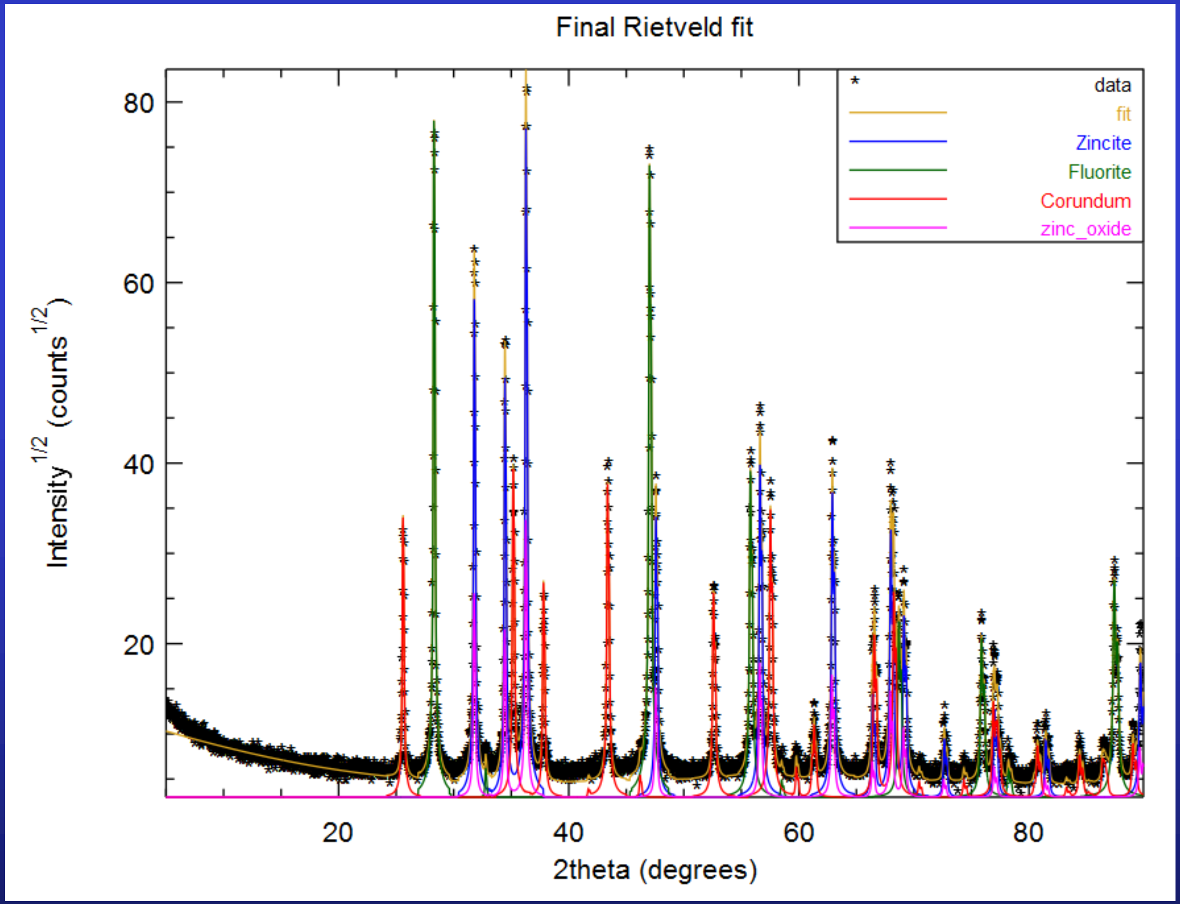

Line Broadening:

Crystallite sizes, shapes, μstrains, distributions

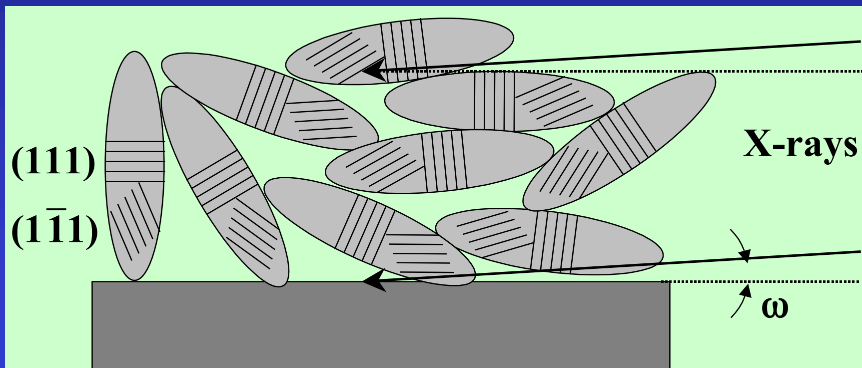

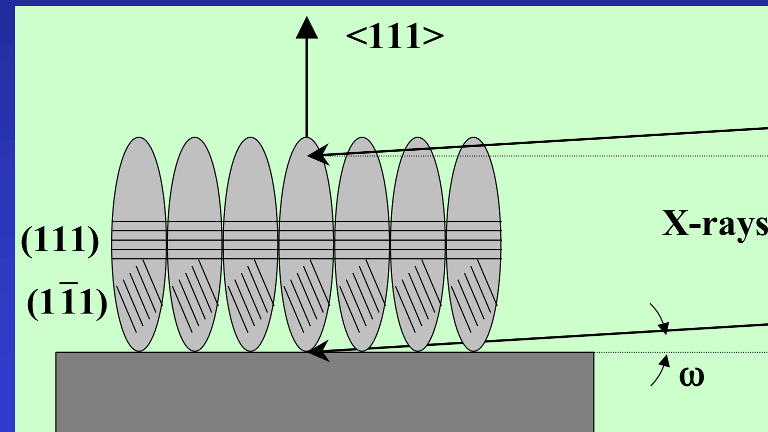

- Texture helps the "real" mean shape determination

Symmetrised spherical harmonics

$$\langle R_{\vec{h}} \rangle = \sum_{\ell=0}^{L} \sum_{m=0}^{\ell} R_\ell^m K_\ell^m(\chi,\varphi)$$

$$K_\ell^m(\chi,\varphi) = P_\ell^m(\cos\chi)\cos(m\varphi) + P_\ell^m(\cos\chi)\sin(m\varphi)$$

$$\langle R_{\mathbf{h}} \rangle = R_0 + R_1P_2^{\,0}(x) + R_2P_2^{\,1}(x)\cos\varphi + R_3P_2^{\,1}(x)\sin\varphi + R_4P_2^{\,2}(x)\cos2\varphi + R_5P_2^{\,2}(x)\sin2\varphi + \ldots$$

$$\langle \varepsilon_{\mathbf{h}}^{\,2} \rangle E_{\mathbf{h}}^{\,4} = E_1h^4 + E_2k^4 + E_3\ell^4 + 2E_4h^2k^2 + 2E_5\ell^2k^2 + 2E_6h^2\ell^2 + 4E_7h^3k + 4E_8h^3\ell + 4E_9k^3h + 4E_{10}k^3\ell + 4E_{11}\ell^3h + 4E_{12}\ell^3k + 4E_{13}h^2k\ell + 4E_{14}k^2h\ell + 4E_{15}\ell^2kh$$

$\bar{1}$

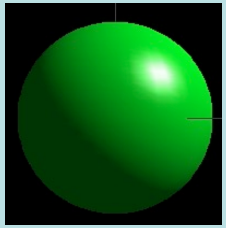

R_0

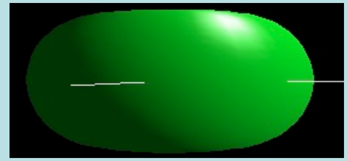

R_0, $R_1 < 0$

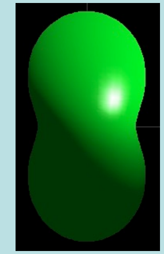

R_0, $R_1 > 0$

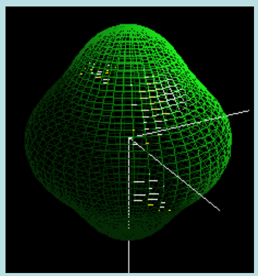

R_0, $R_6 > 0$

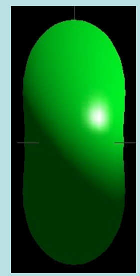

R_0,
R_2 and $R_6 > 0$

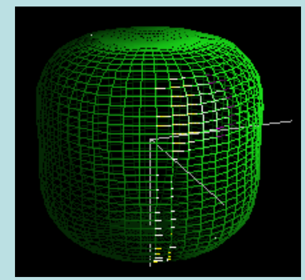

R_0, $R_6 < 0$

6/m

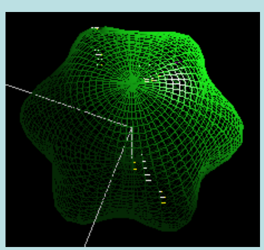

R_0, $R_4 > 0$

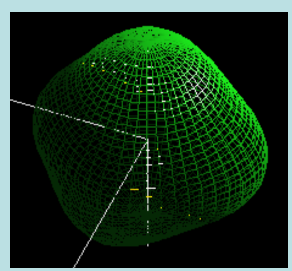

R_0, $R_1 > 0$

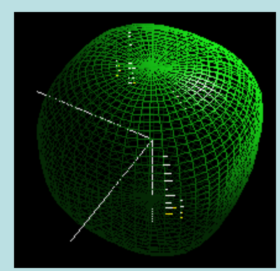

R_0, $R_1 < 0$

m3m

EMT nanocrystalline zeolite

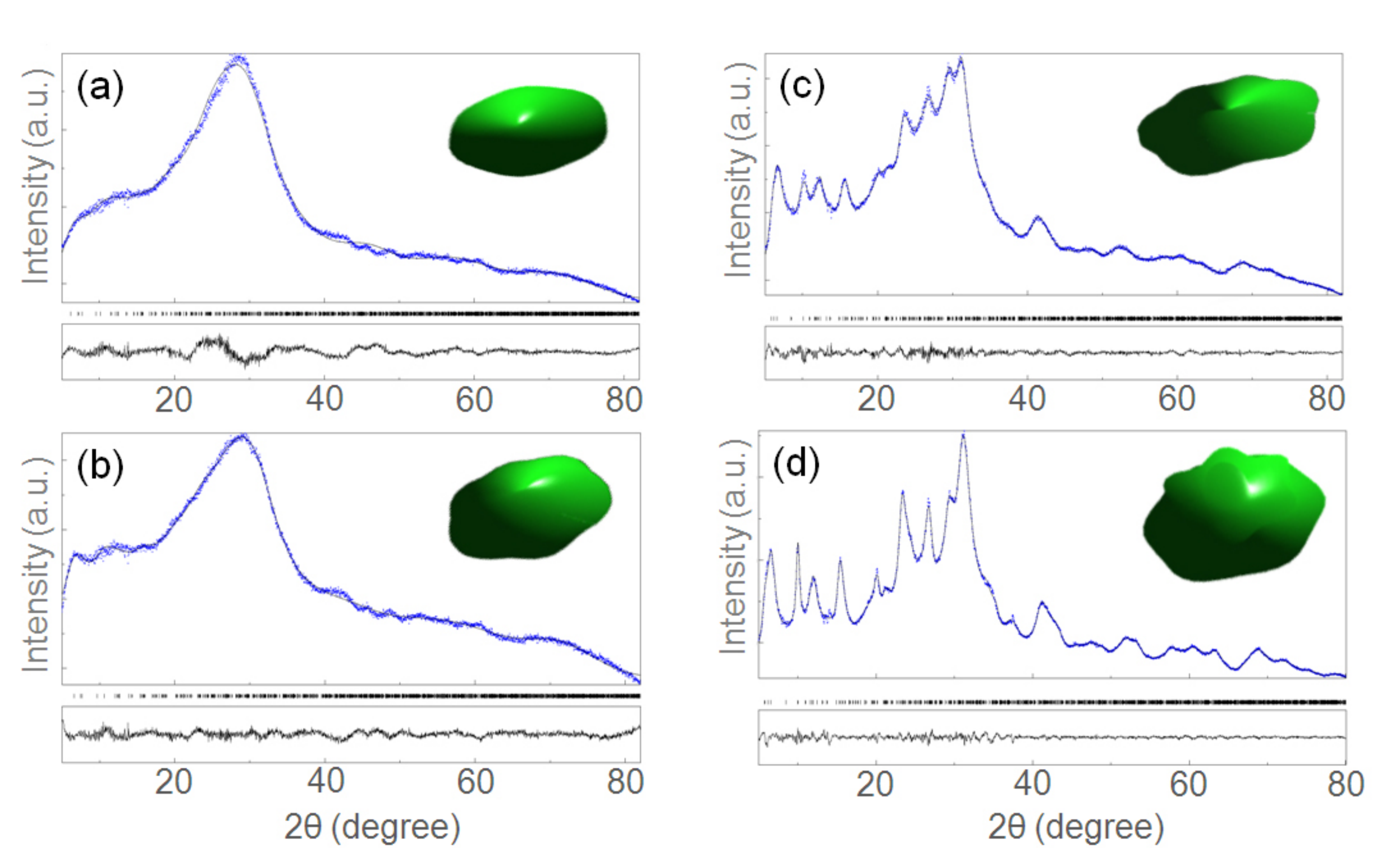

Ng, Chateigner, Valtchev, Mintova: *Science* **335** (2012) 70

Irradiated FluorApatite (FAp) ceramics

Self-recrystallisation under irradiation, depending on SiO_4 / PO_4 ratio (FAp / Nd-Britholite) and on irradiating species

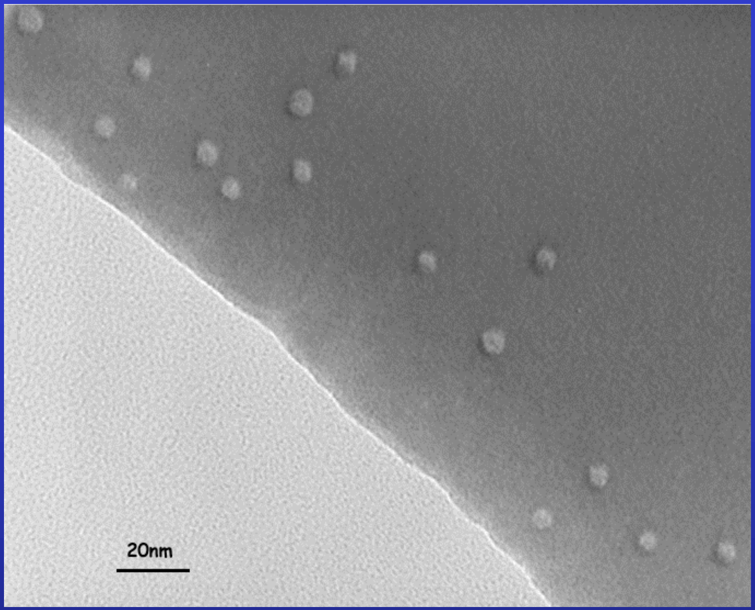

TEM of FAp irradiated with 70 MeV, 10^{12} Kr cm^{-2} ions

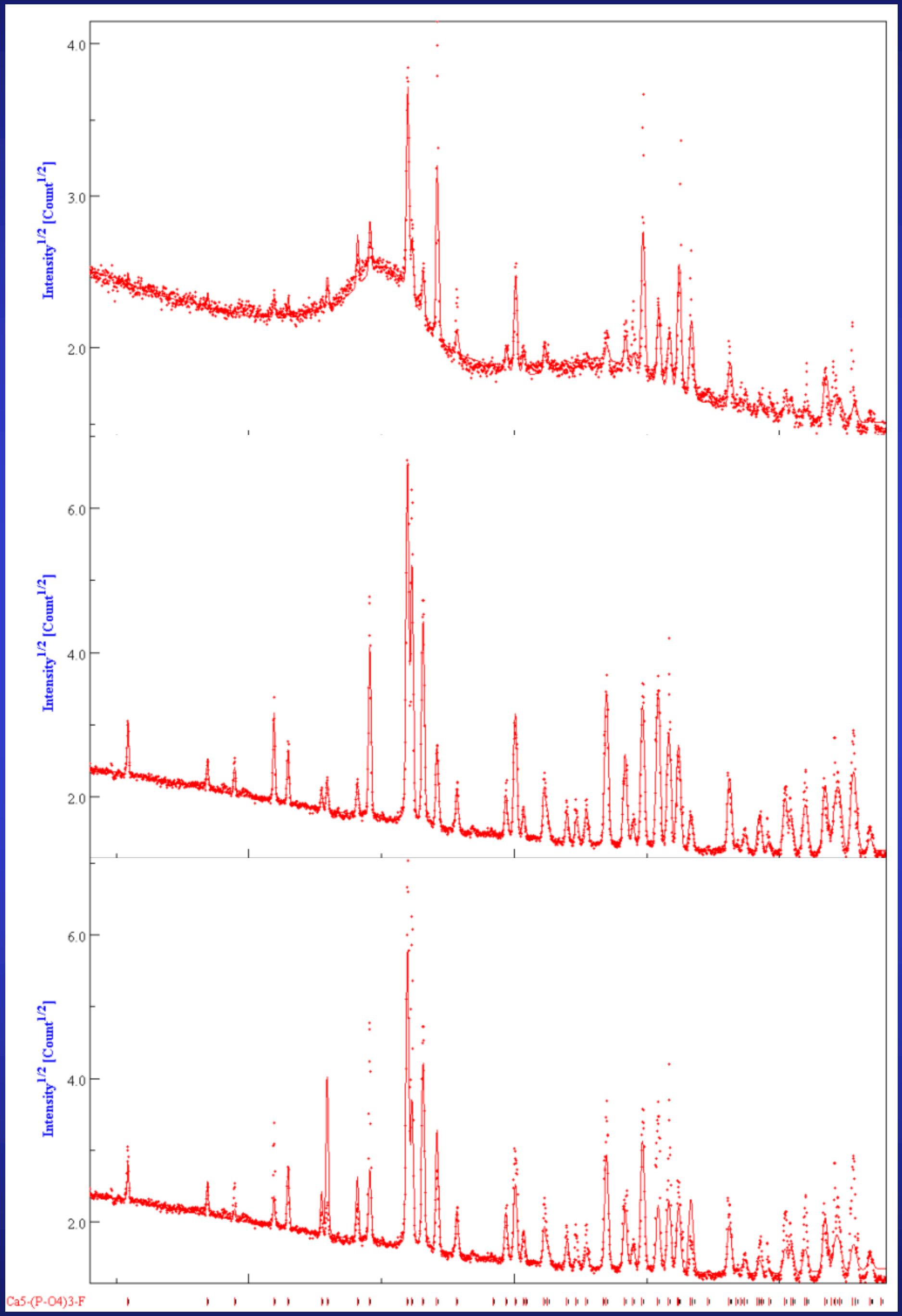

texture corrected,

10^{13} Kr cm^{-2}

Virgin, with texture correction

Virgin, no texture correction

Fluence (ions.cm^{-2})	Vc/V (%)	A (Å)	c (Å)	<t> (nm)	$\Delta a/a_0$ (%)	$\Delta c/c_0$ (%)	R_w (%)	R_B (%)
0	100	9.3365(3)	6,8560(5)	294(22)	-	-	14.6	9.1
Kr								
10^{11}	100	-	-	-	-	-		
10^{12}	100	-	-	-	-	-		
5.10^{12}	49(1)	9.3775(9)	6.8912(8)	294(20)	0.44	0.53	24	15
10^{13}	20(1)	9.4236(5)	6.9105(5)	291(20)	0.94	0.82	9.9	6
5.10^{13}	14(1)	9.3160(4)	6.8402(5)	294(22)	-0.21	-0.22	10.5	5.9
I								
10^{11}	-	-	-	-	-	-		
5.10^{11}	86(2)	9.3603(3)	6.8790(5)	90(10)	0.26	0.35	23.9	15.1
10^{12}	-	-	-	-	-	-		
3.10^{12}	47(2)	9.3645(3)	6.8840(5)	91(6)	0.30	0.42	13.3	9
5.10^{12}	29.2(5)	9.3765(5)	6.8881(6)	77(11)	0.44	0.48	10.4	7.3
10^{13}	13.2(2)	9.3719(4)	6.8857(6)	82(9)	0.38	0.45	6.7	4.9

Single impact model associated to crystal size reduction

Cell parameters and volume increase, then relax

Amorphisation / recrystallisation competition: single or double impact

Amorphous/crystalline volume fraction (damaged fraction Fd = Va / V) as determined by x-ray diffraction

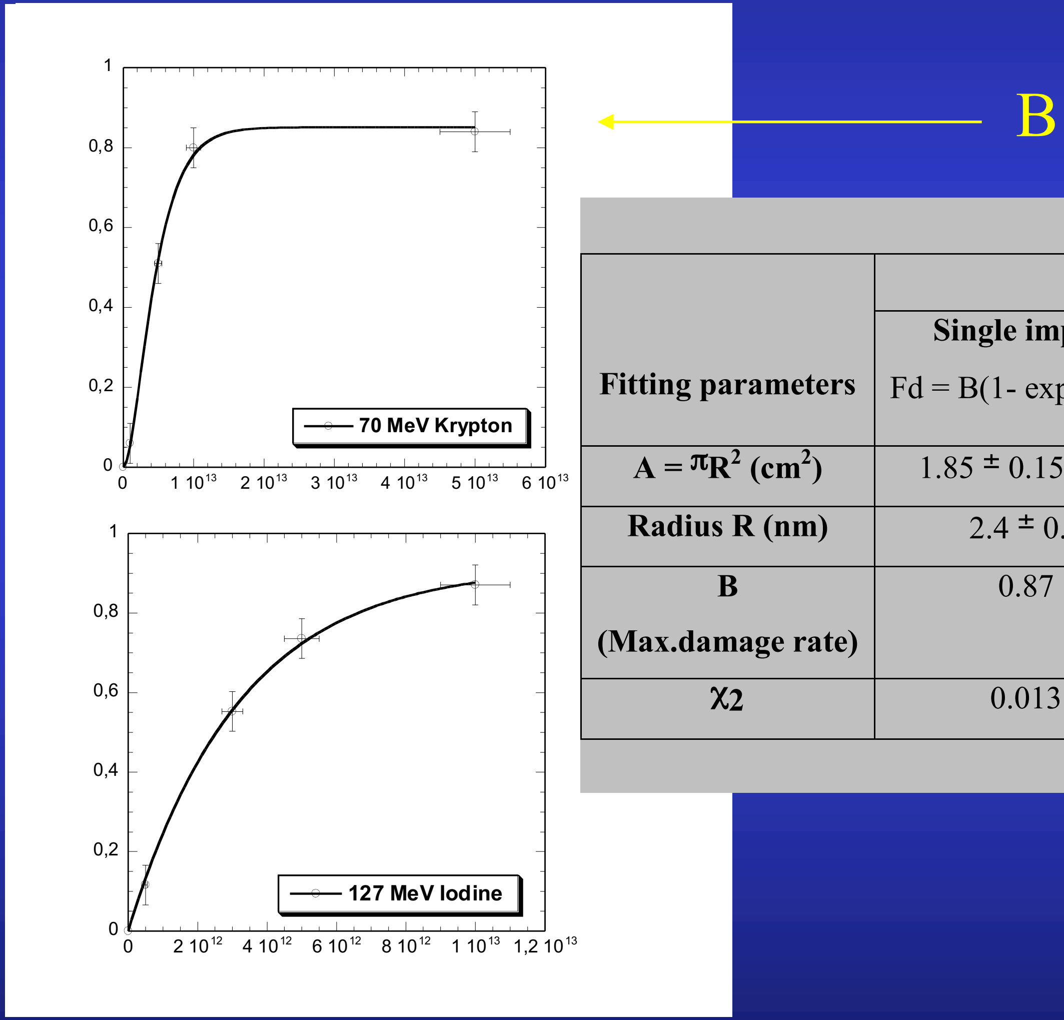

Fitting parameters	Krypton		Iodine
	Single impact $Fd = B(1- \exp(-A\phi t))$	Double impact $Fd = B(1 - (1+ A\phi t) \exp(-A\phi t))$	Single impact $Fd = B(1- \exp(-A\phi t))$
$A = \pi R^2$ (cm^2)	$1.85 \pm 0.15\ 10^{-13}$	$4.1 \pm 0.15\ 10^{-13}$	$3.3 \pm 0.15\ 10^{-13}$
Radius R (nm)	2.4 ± 0.2	3.6	3.2
B (Max.damage rate)	0.87	0.85 ± 0.2	0.92 ± 0.2
$\chi 2$	0.013	0.0006	0.0004

Mullite-silica composites

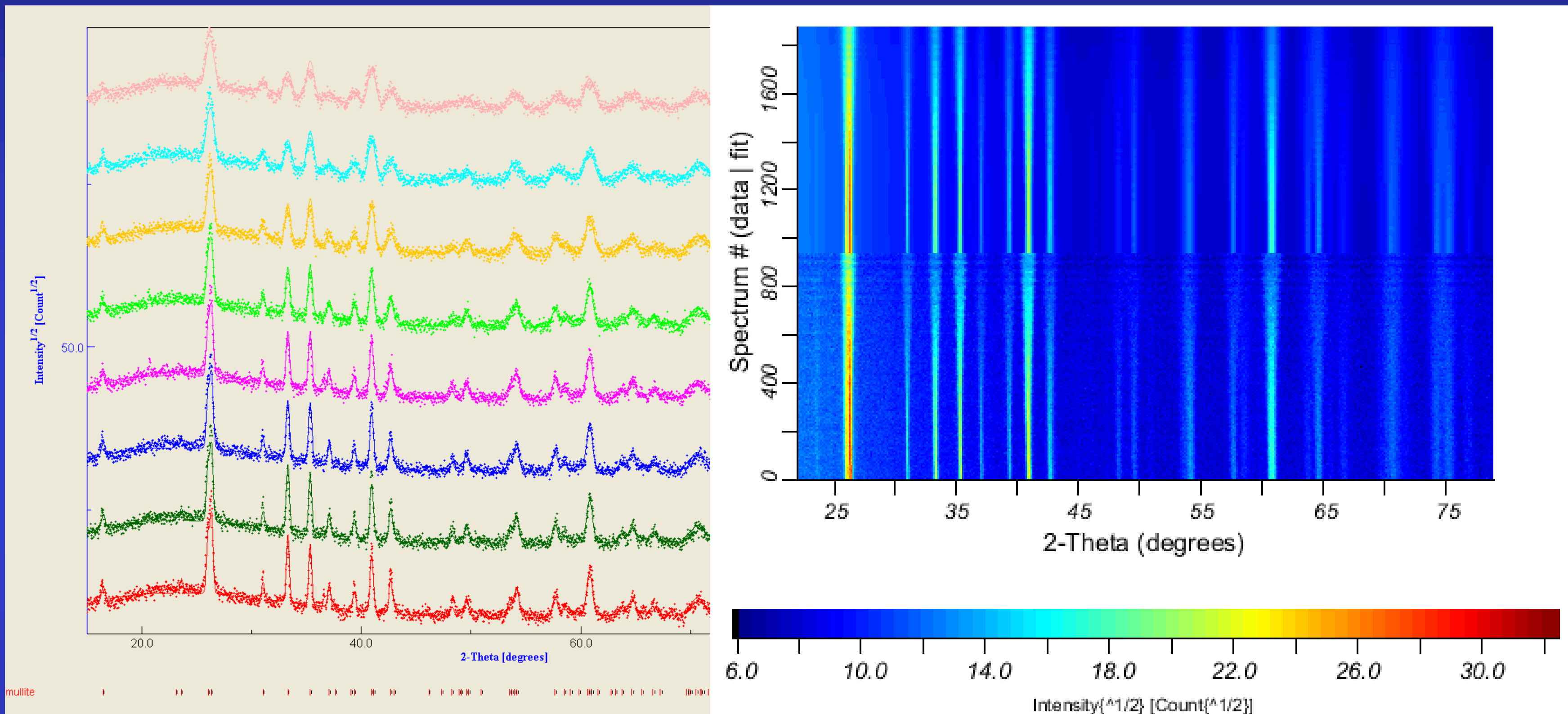

ODF: R_w = 4.87 %, R_B = 4.01 %

Rietveld: R_w = 12.90 %, GoF = 1.77

Mullite: a = 7.56486(5) Å; b = 7.71048(5) Å; c = 2.89059(1)Å

Uniaxially pressed

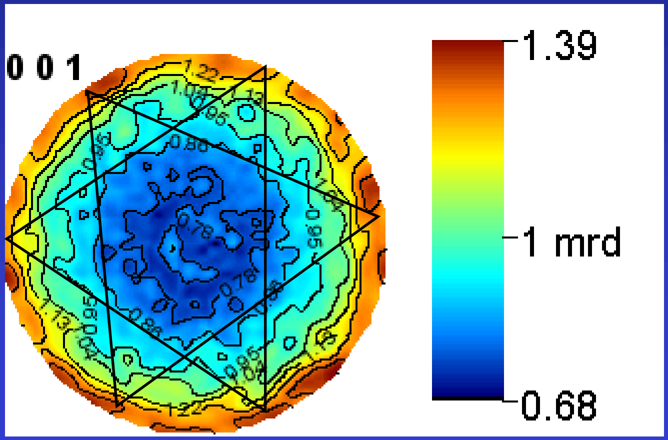

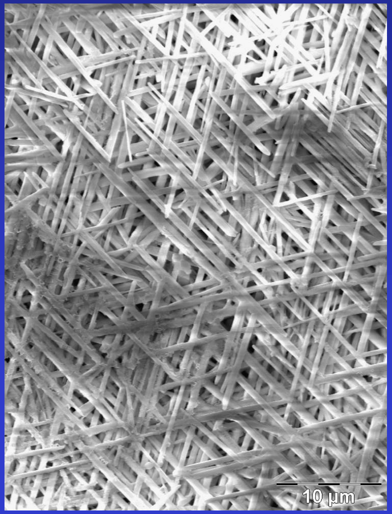

Centrifugated

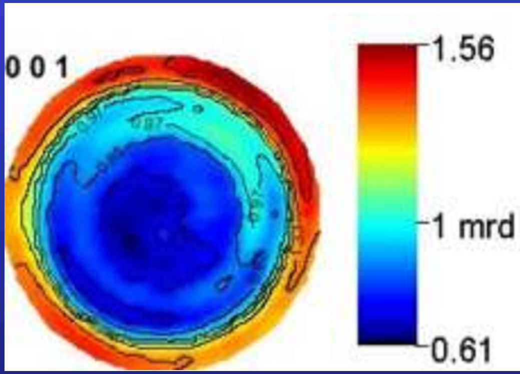

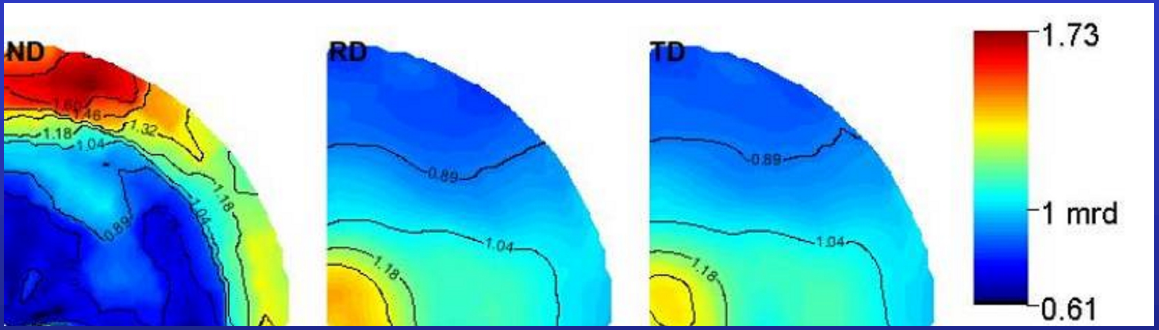

Texture of amphiboles collected at ≠ places and in ≠ lithologic types

↳ **White mica and chlorite partially replace amphibole or fill small fractures with quartz and carbonates**

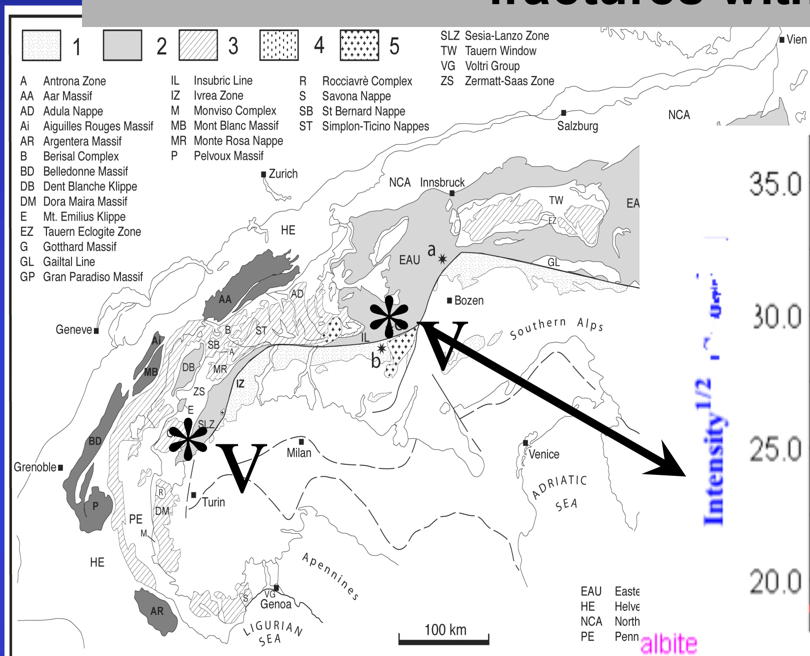

Fig. 1* –Tectonic sketch map of the Alpine chain: shaded areas correspond to continental Alpine crust. Legend: 1 = Southalpine basement; 2 = Austro
4 = Helvetic basement; 5=Tertiary intrusive stocks. Stars localise the Texel Gruppe metapelites in the Oetztal nappe (a), the Eastern Orobic Alps metap
(b) and the Mortirolo Pass area in Central Austroalpine domain of the Languard-Campo Nappe (c).

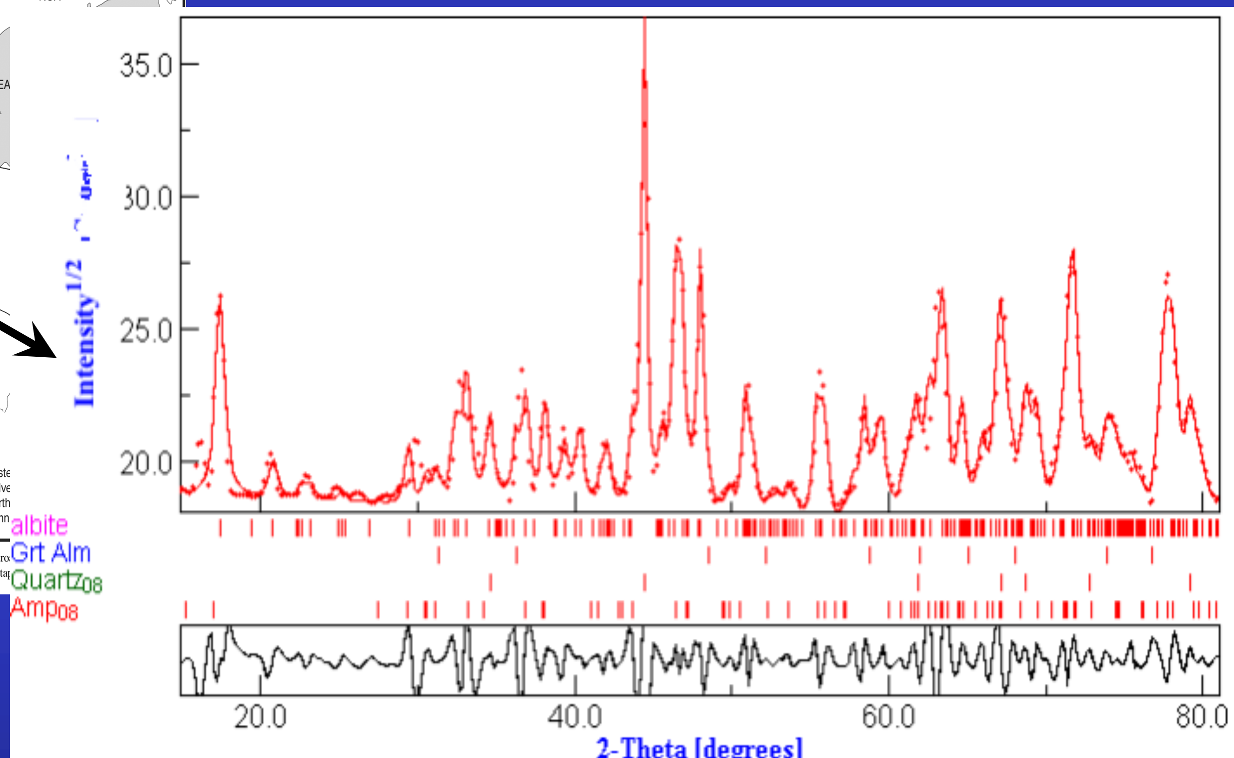

Combined approach allows to access pole figures for most of the rock-forming minerals (even for mica)

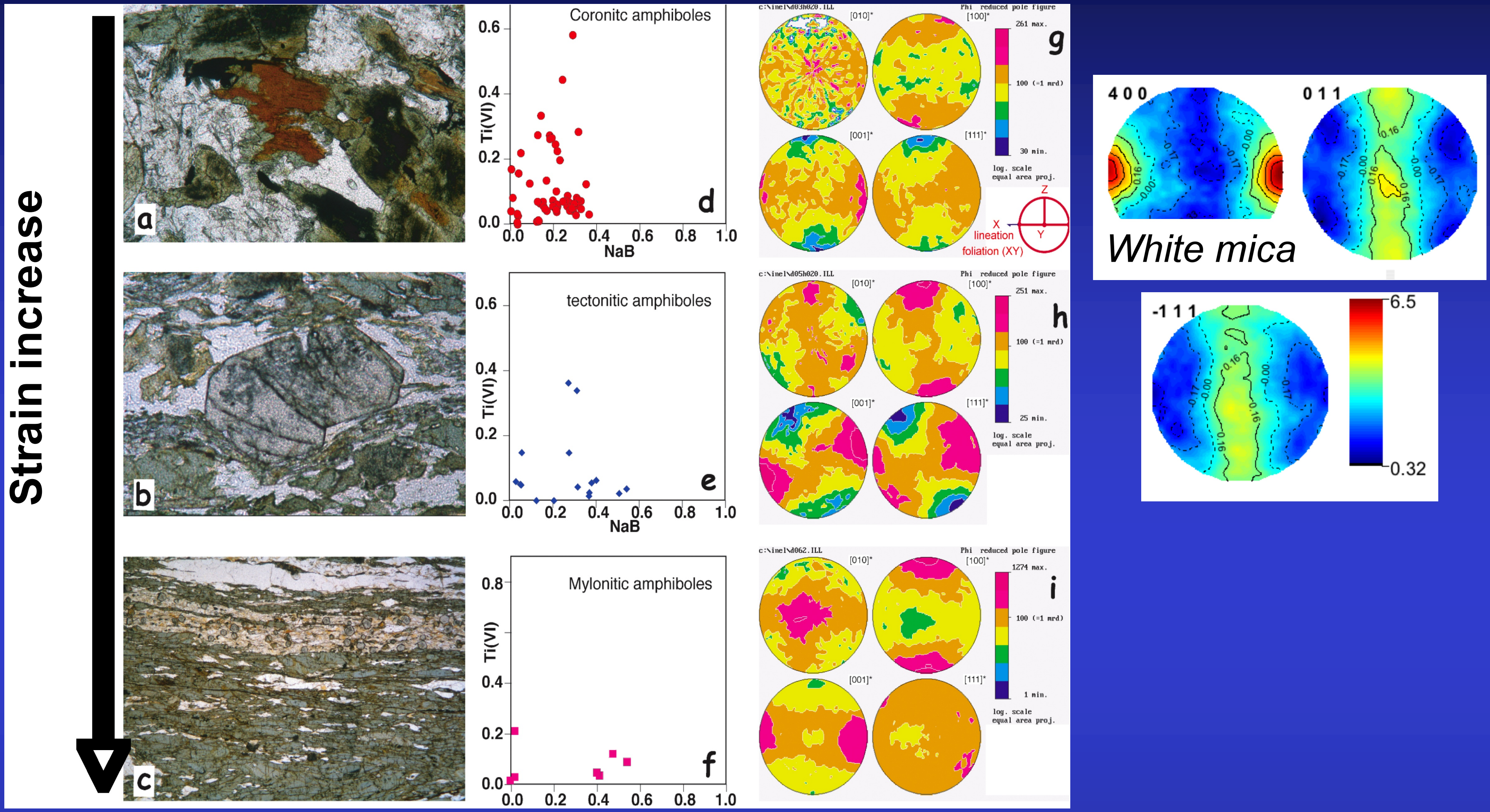

Degree of fabric evolution due to:

- deformation partitioning at metric-scale

- degree of chemical changes within amphiboles

- evolving metamorphic conditions during Alpine subduction (60-100 Million years).

Carbon nanofibre

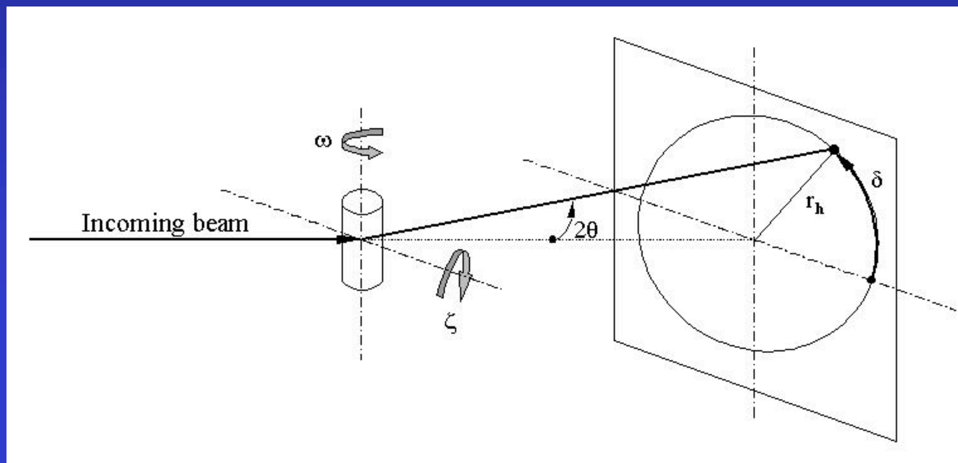

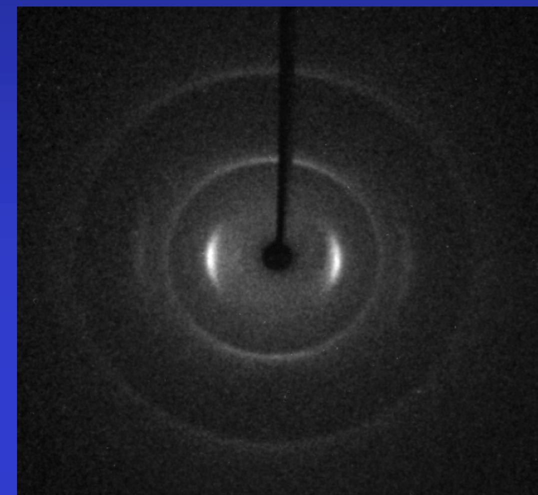

1 fibre (7 microns diameter): CCD Kappa diffractometer

Planar texture Component
Ufer turbostratic model

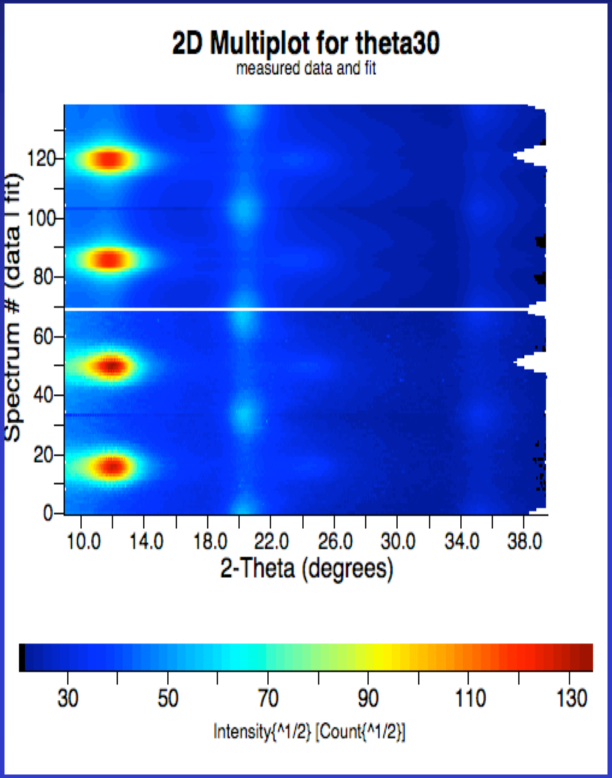

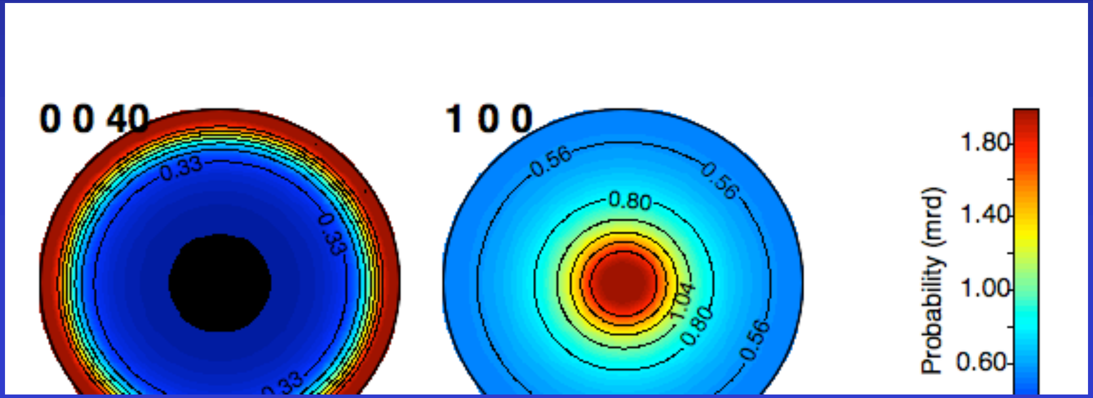

	A(nm)	C(nm)	Orientation FWHM(°)	Max 00l pole figure (m.r.d.)	Crystallite size along c (nm)	Crystallite size along a (nm)	Global microstrain (rms)
C1B1	0.23589(7)	0.6821(1)	21.6(1)	1.95	2.1(4)	2.2(4)	0.0152(10)
C2B1	0.23746(5)	0.68915(8)	18.75(6)	2.05	2.3(2)	2.5(2)	0.0154(11)
C3B1	0.23734(5)	0.69233(9)	18.63(6)	2.04	2.4(3)	2.7(5)	0.0136(6)
C3B2	0.23716(4)	0.69389(9)	19.87(7)	1.98	2.4(4)	2.5(4)	0.0150(4)
C3B3	0.23656(4)	0.68980(8)	19.16(6)	1.99	2.5(6)	2.3(5)	0.0168(8)

Turbostratic phyllosilicate aggregates

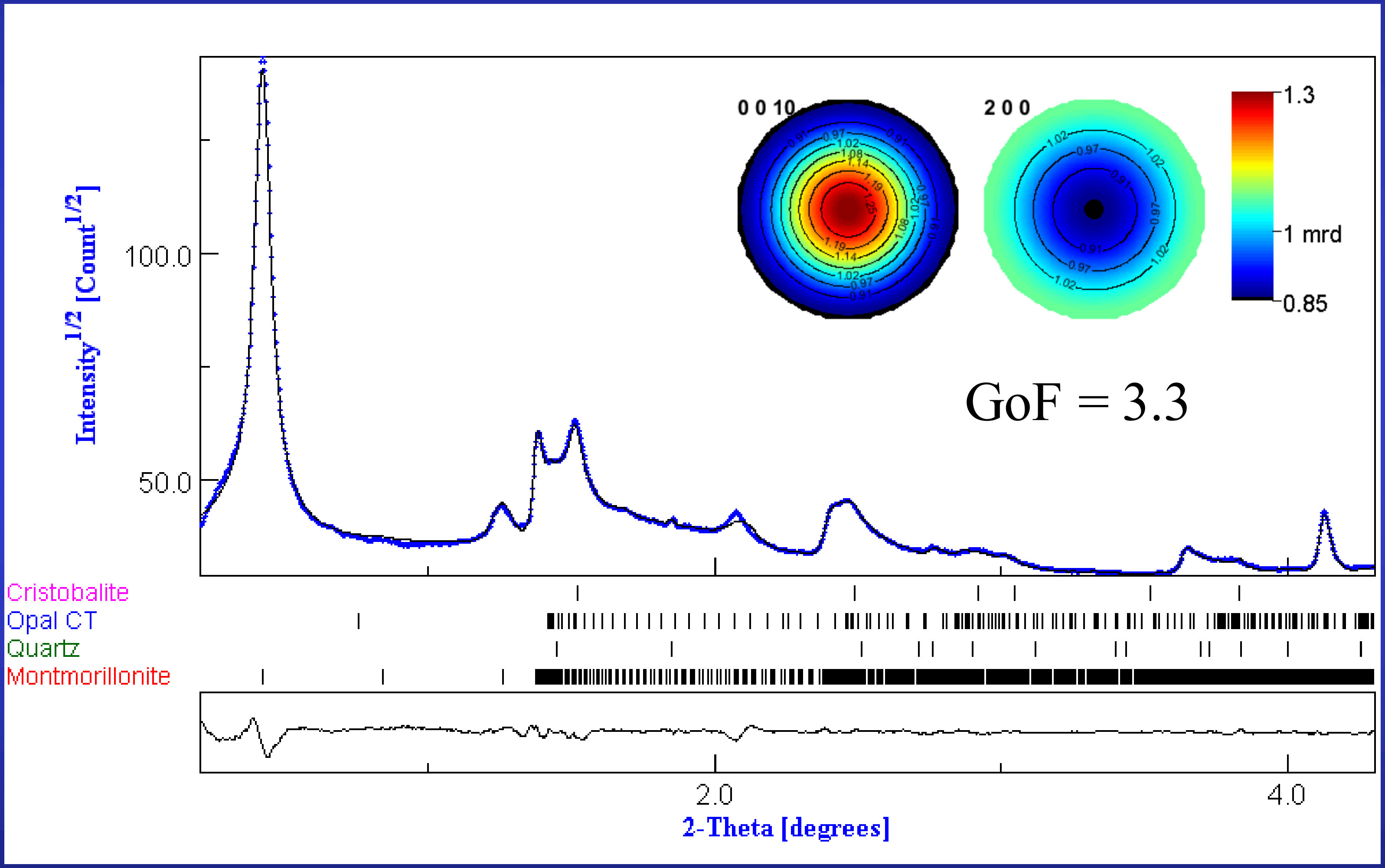

V%
1.45(2)
6.6(1)
0.19(1)
91.8(3)

$Mg_{0.75}Fe_{0.25}O$ high pressure experiments

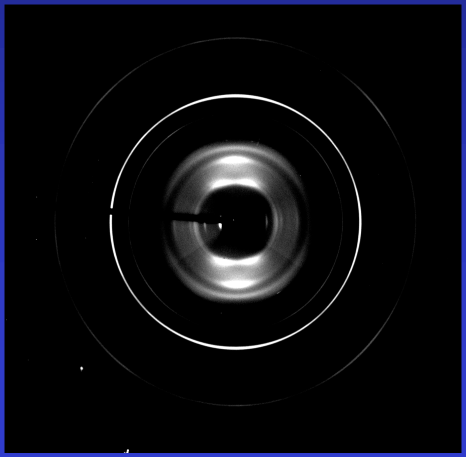

E-WIMV + geo

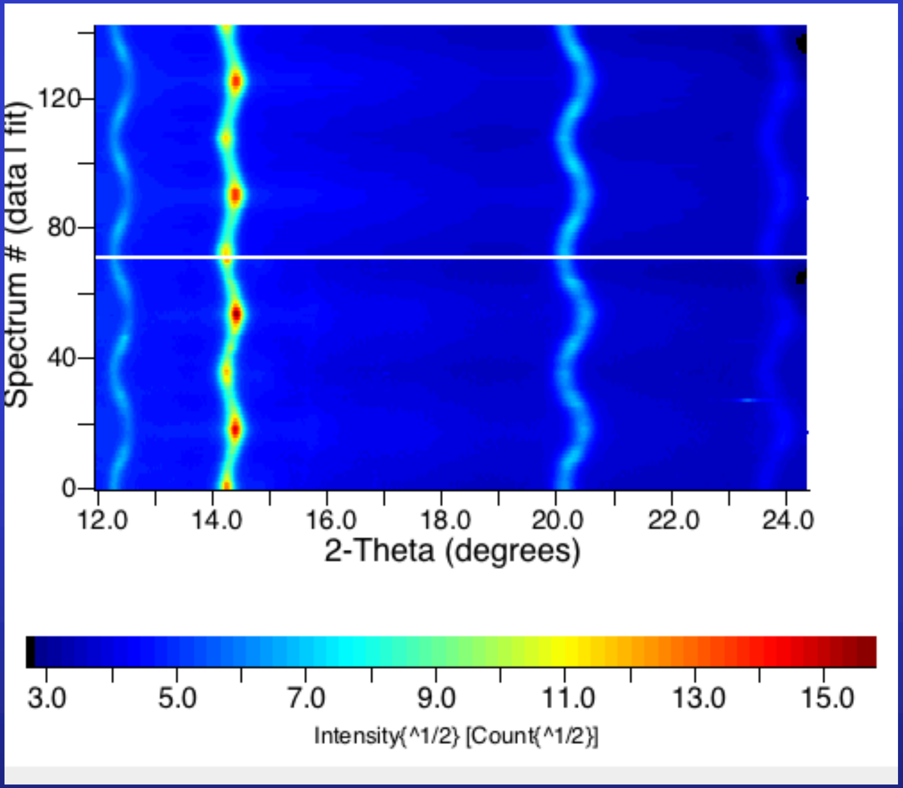

a = 3.98639(3) Å

<t> = 46.8(3) Å

<ε> = 0.00535(1)

σ_{33} = -861(3) MPa

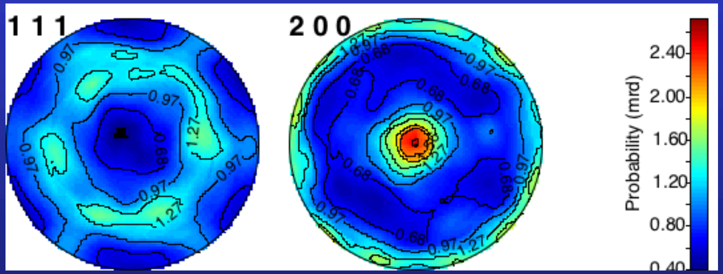

$LiNbO_3$

- Predict macroscopic anisotropic properties: BAW

Propagation equation

$$\rho \frac{\partial^2 u^i}{\partial t^2} = \left[\mathrm{C}^{i\ell mn} \right] \frac{\partial^2 u_n}{\partial x^m \partial x^\ell}$$

Propagation direction	V_P	V_{S1}	V_{S2}
[100]	$\sqrt{\frac{c^M{}_{11}}{\rho}}$	$\sqrt{\frac{c^M{}_{44}}{\rho}}$	$\sqrt{\frac{c^M{}_{44}}{\rho}}$
[110]	$\sqrt{\frac{c^M{}_{11} + 2c^M{}_{44} + c^M{}_{12}}{2\rho}}$	$\sqrt{\frac{c^M{}_{11} - c^M{}_{12}}{2\rho}}$	$\sqrt{\frac{c^M{}_{44}}{\rho}}$
[111]	$\sqrt{\frac{c^M{}_{11} + 4c^M{}_{44} + 2c^M{}_{12}}{3\rho}}$	$\sqrt{\frac{c^M{}_{11} + c^M{}_{44} - c^M{}_{12}}{3\rho}}$	$\sqrt{\frac{c^M{}_{11} + c^M{}_{44} - c^M{}_{12}}{3\rho}}$

Cubic crystal system

	c_{11} or c_{11}^M	c_{12} or c_{12}^M	c_{13} or c_{13}^M	c_{14} or c_{14}^M	c_{33} or c_{33}^M	c_{44} or c_{44}^M
Single crystal	201	54.52	71.43	8.4	246.5	60.55
$LiNbO_3$/Si	206.4	68.5	67.6	0.48	216.5	64
$LiNbO_3$/Al_2O_3	204	65.7	69.7	1.1	219.9	63.2

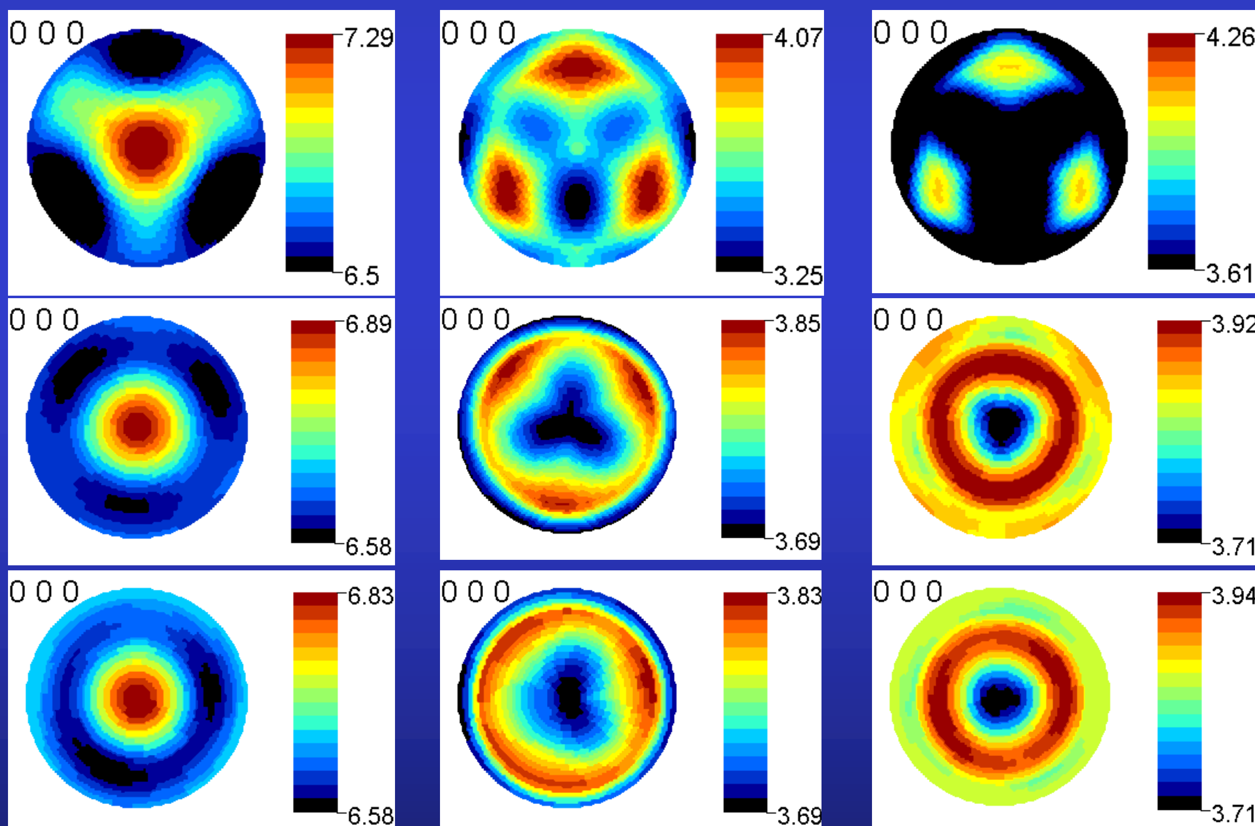

Single crystal

$LiNbO_3$/Si

$LiNbO_3$/Al_2O_3

$ErMn_3Fe_9C$ ferrimagnet

Predict macroscopic anisotropic properties: Magnetisation

$$\frac{M_\perp}{M_S} = 2\pi \int_0^{\frac{\pi}{2}} (1-\rho_0) PV(\theta_g) \sin\theta_g \cos(\theta_g - \theta)\, d\theta_g + \rho_0 M_{random}$$

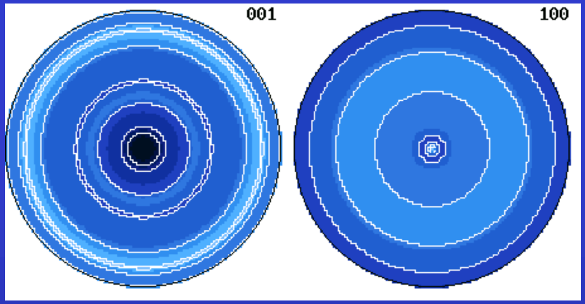

max {001}: 3.9 mrd
min: 0.5 mrd

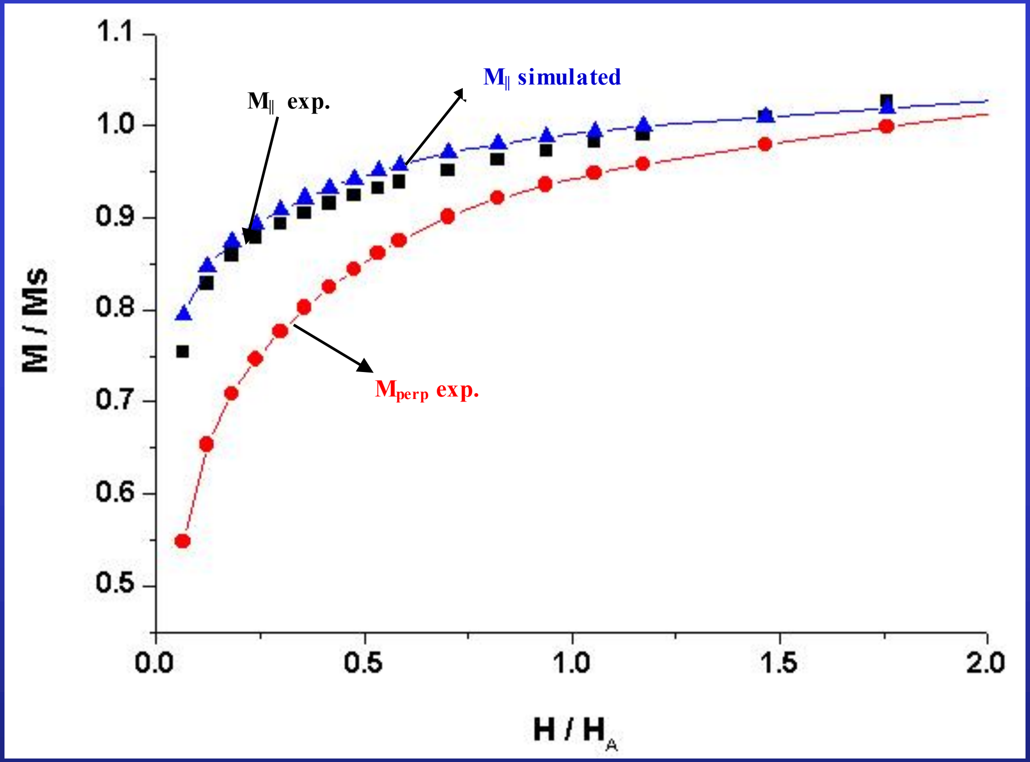

EDP Combined Analysis

QTA: local vs global | Pt thin film on Si

a) 6 µm diameter selected area, b) EPD and c) 2D plot.

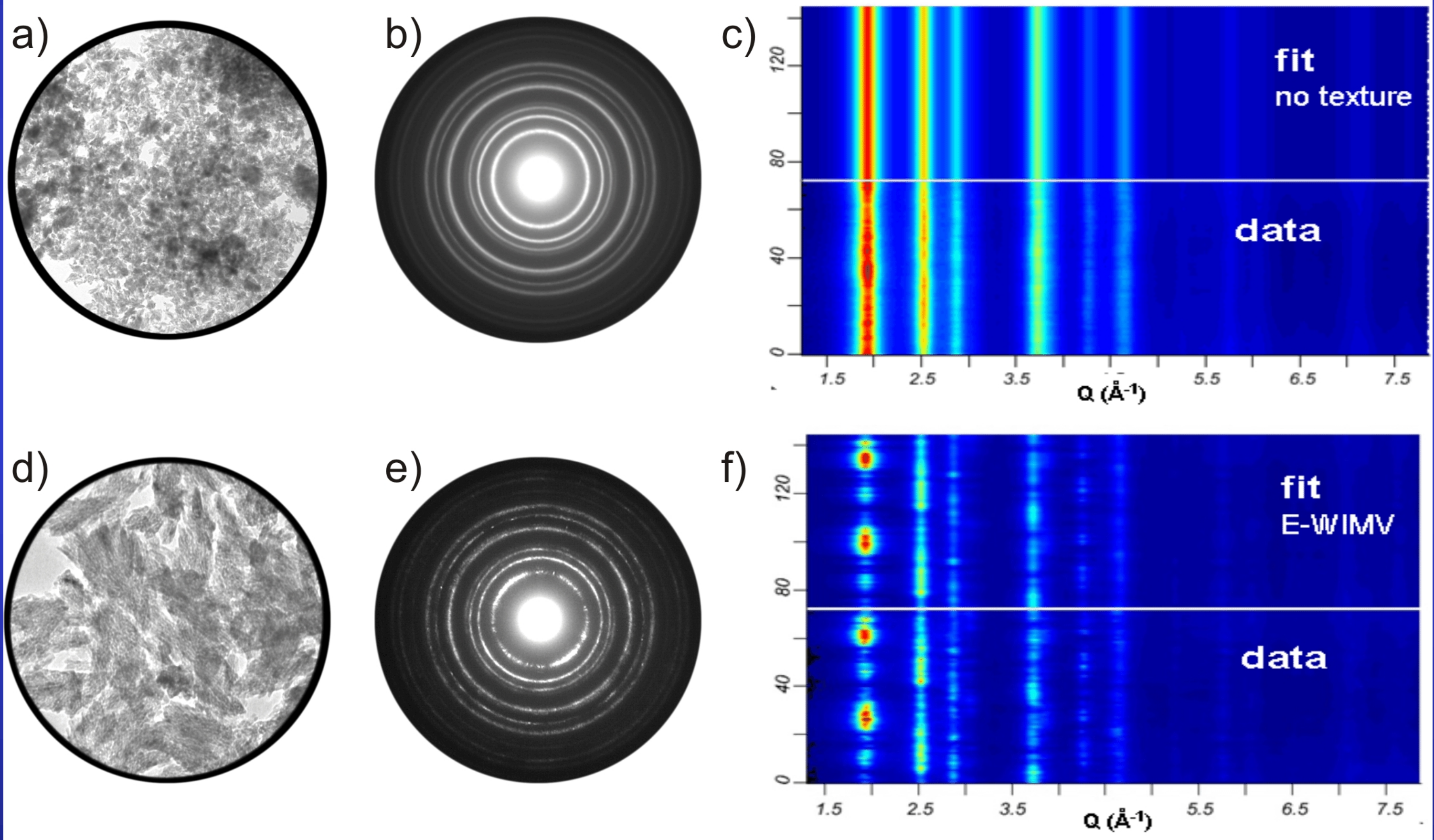

d) 0.5 µm diameter selected area, e) EPD and f) 2D plot

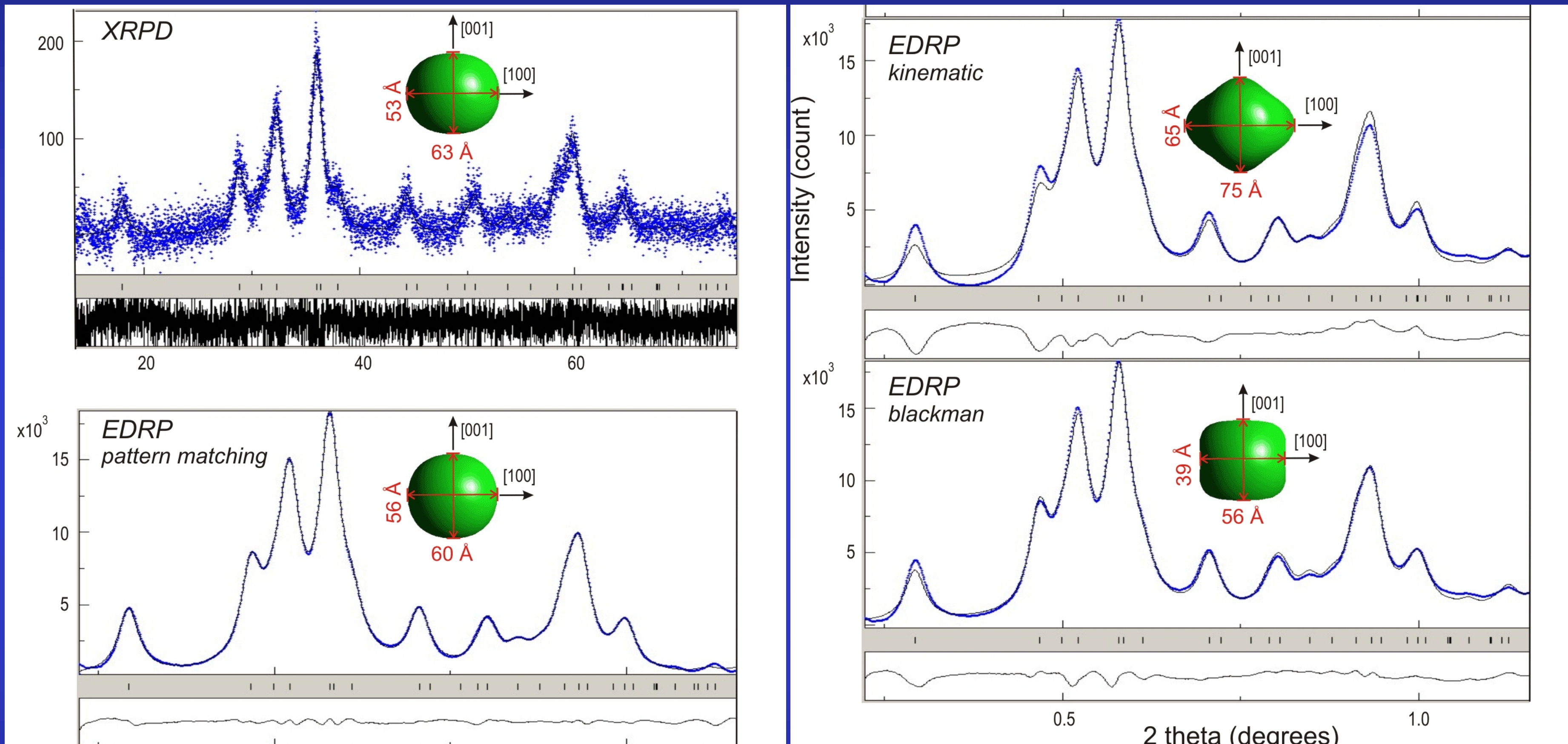
XRPD
200
100
[001]
[100]
53 Å
63 Å
20
40
60
EDRP
pattern matching
x10³
15
10
5
56 Å
60 Å
EDRP
kinematic
65 Å
75 Å
EDRP
blackman
39 Å
56 Å
Intensity (count)
0.5
1.0
2 theta (degrees)

Combined XRR, XRD & GiXRF Analysis

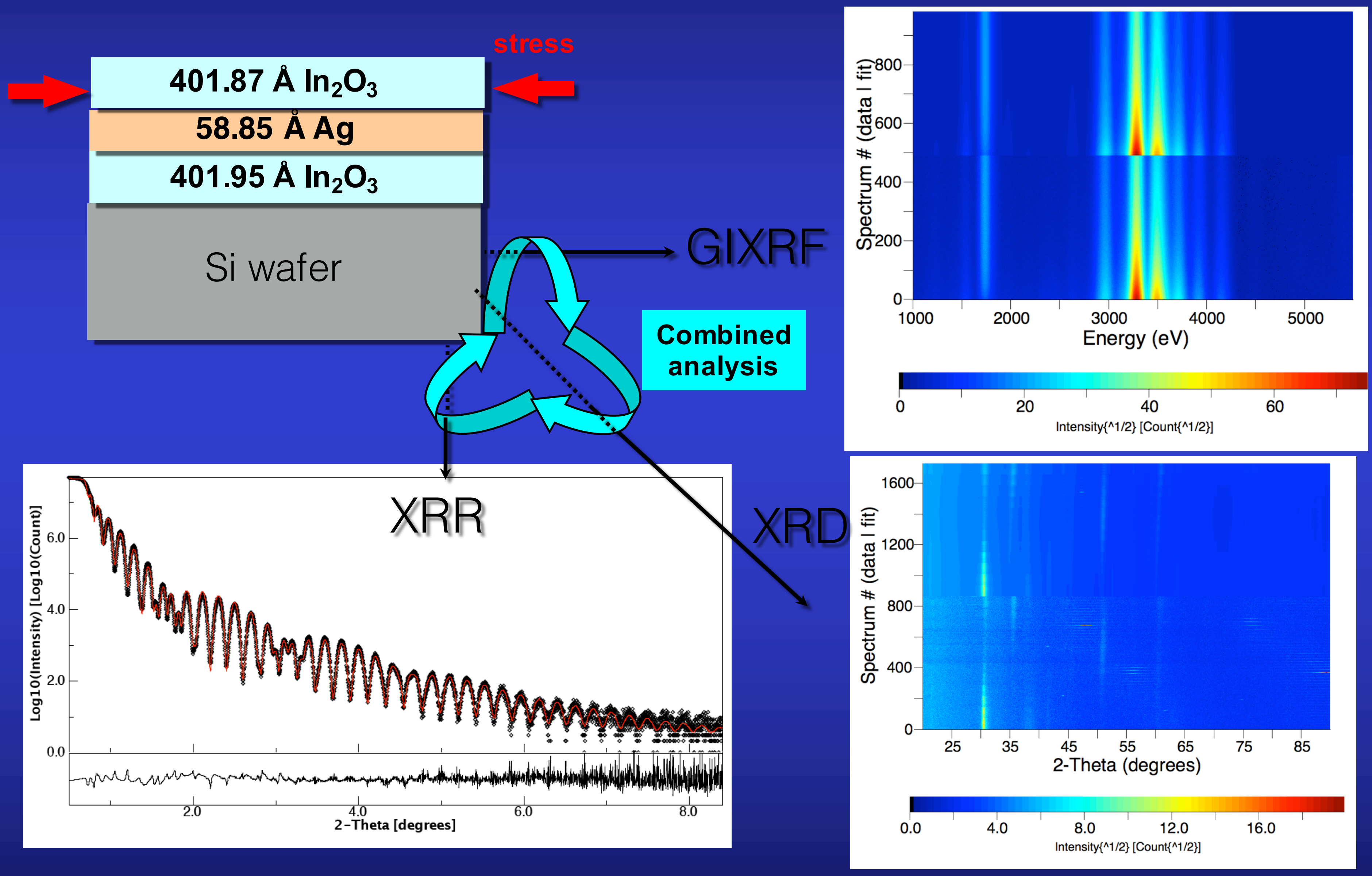

XRR

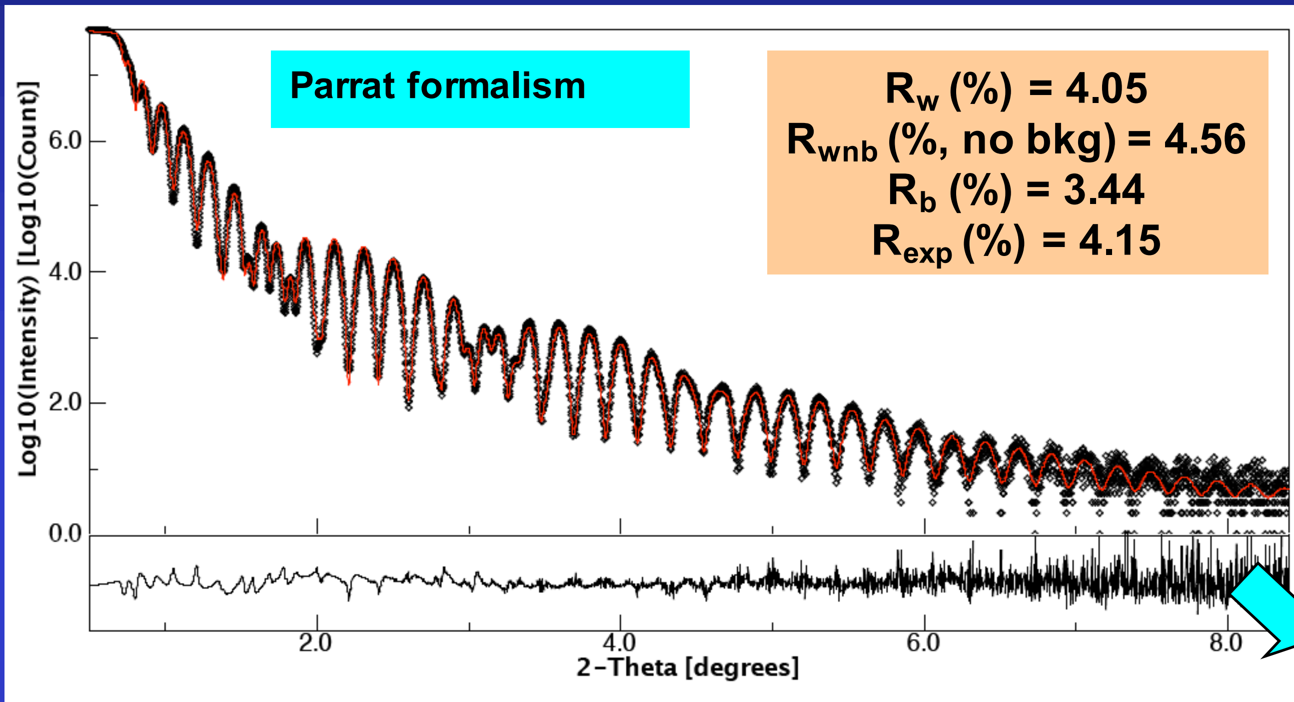

Highly porous In_2O_3 layer

Top layer: q_c = 0.0294 $Å^{-1}$; roughness r =0.38nm

Top In_2O_3: q_c = 0.0504 $Å^{-1}$; r =2.06 nm

Ag : q_c = 0.0576 $Å^{-1}$; r =0.26 nm

Bottom In_2O_3: q_c = 0.04889 $Å^{-1}$; r =6.74 nm

Si wafer: q_c = 0.0313 $Å^{-1}$; r = 0.73 nm

XRD

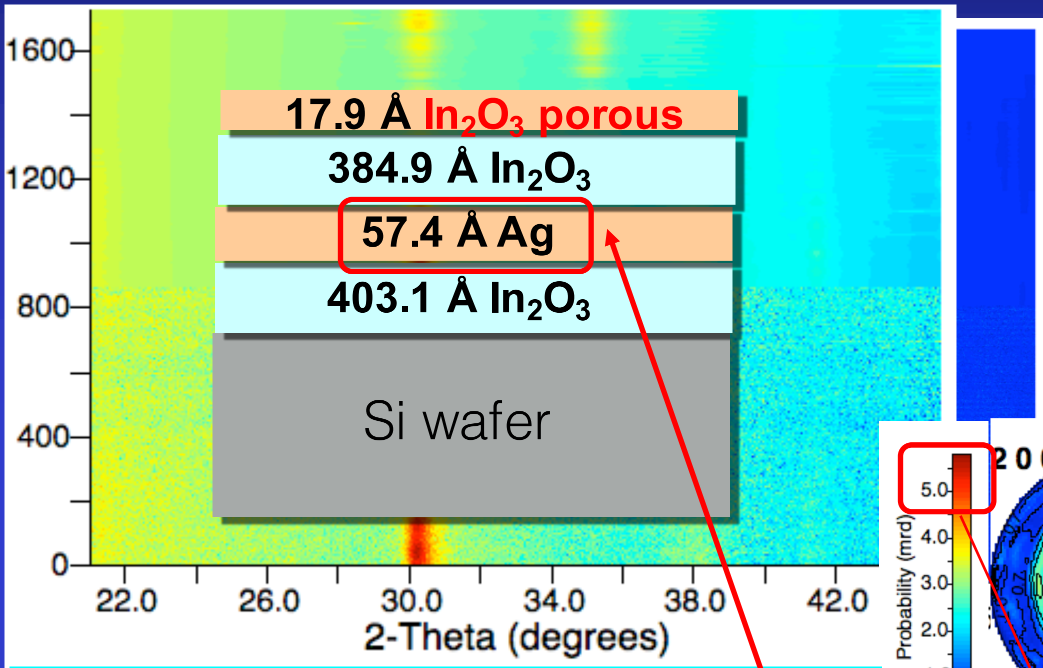

R_w (%) = 23.97
R_{wnb} (%, no bkg) = 58.31
R_b (%) = 18.71
R_{exp} (%) = 22.04

Refined Ag phase parameters

- Isotropic crystallite size = 56.4 (1.3) Å
- Cell parameter: a = 4.0943(7) Å

In_2O_3

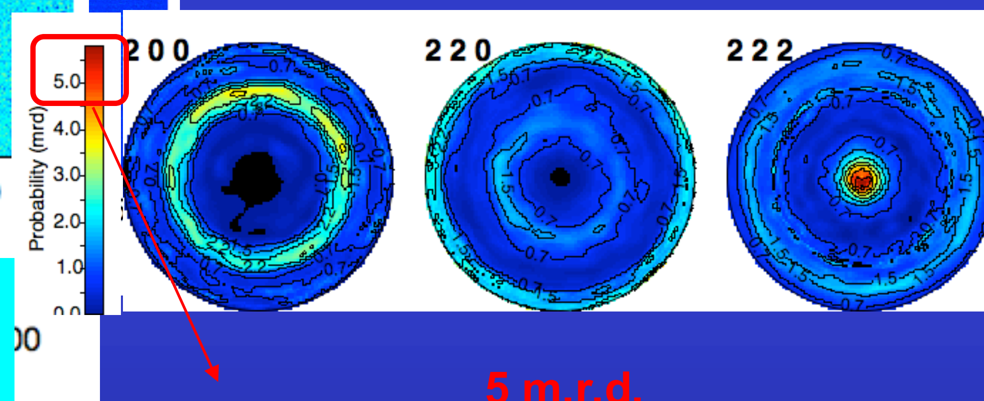

5 m.r.d.

Ag:

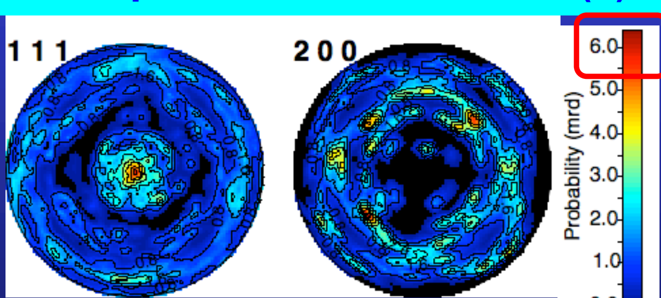

Refined In_2O_3 phase parameters

- σ_{XX} = - 1 GPa (in-plane compressive stress)
- Isotropic crystallite size = 153.2(5) Å
- Cell parameter: a = 10.2104(5) Å

GiXRF

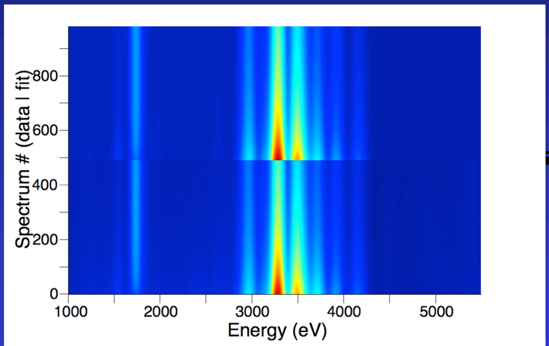

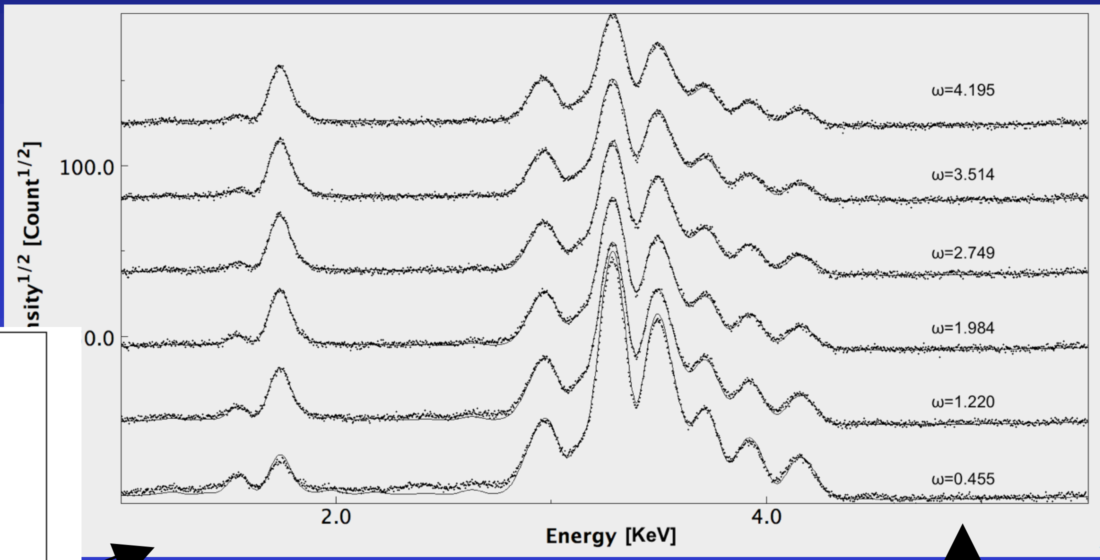

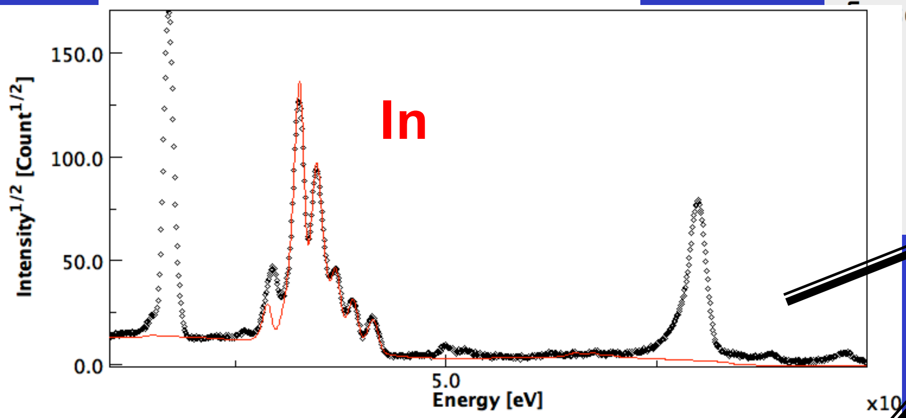

No presence of contaminant observed

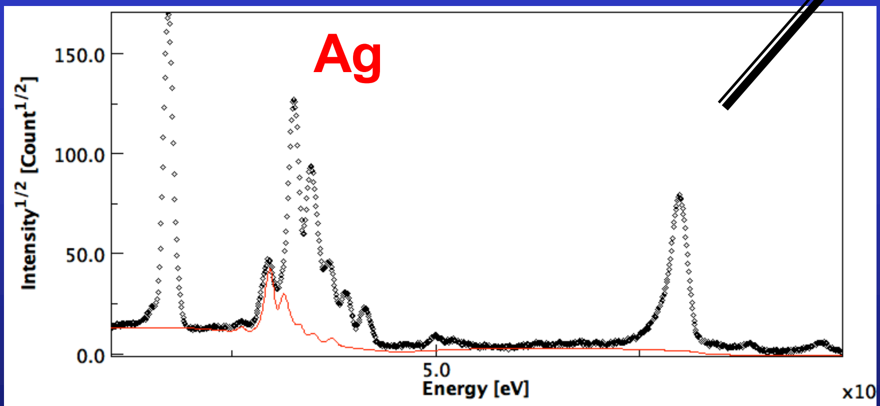

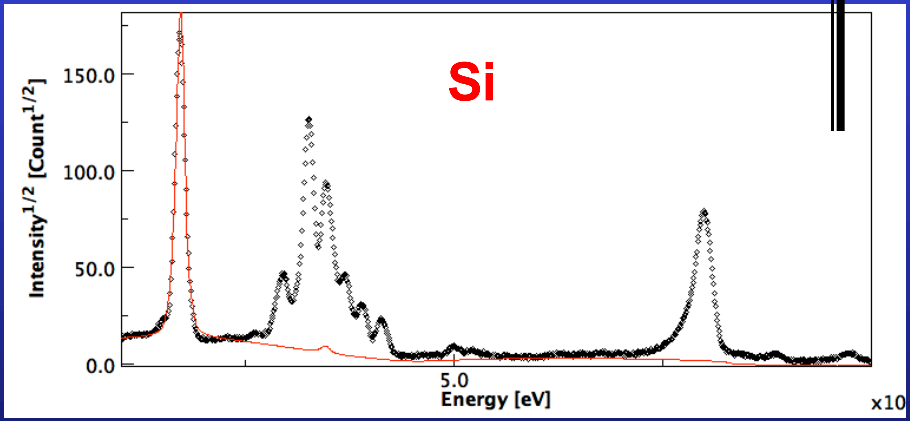

XRD-XRF-Raman-IR Combined Analysis

$$I_{aj} = \frac{\lambda}{hc} C_{aj} \frac{\tau_{aj}}{\mu_{j\lambda}/\rho_j} J_{aj} \omega_a g_a exp\left\{-\sum_{n=1}^{j-1} \frac{\mu_{na} d_n}{sin\Psi_d}\right\} S_1 \int_0^{d_j} dz \left(\frac{-\partial P_{jz}}{\partial z}\right) exp\left(\frac{\mu_{ja} z}{sin\Psi_d}\right)$$

IR

XRF-GiXRF-TXRF

Databases:

COD/TCOD

ROD, MPOD

Raman

$$I_{(e_s,e_0)} = I_0 \frac{\hbar}{2\omega_m}(n_m + 1)\frac{(\omega_0 - \omega_m)^4}{c^4}\left|e_s . \alpha_{ij}^m . e_0\right|^2$$

XRR

$$r = \frac{M_{12}}{M_{22}} = \frac{r_{01} + r_{12} e^{-2iq_{1z}h}}{1 + r_{01} r_{12} e^{-2iq_{1z}h}}$$

Diffraction extended Rietveld

$$y_c(\mathbf{y_S},\theta,\eta) = y_b(\mathbf{y_S},\theta,\eta) + I_0 \sum_{i=1}^{N_L} \sum_{\Phi=1}^{N_\Phi} \frac{\nu_{i\Phi}}{V_{c\Phi}^2} \sum_h Lp(\theta) j_{\Phi h} \left|F_{\Phi h}\right|^2 \Omega_{\Phi h}(\mathbf{y_S},\theta,\eta) P_{\Phi h}(\mathbf{y_S},\theta,\eta) A_{i\Phi}(\mathbf{y_S},\theta,\eta)$$

Why not more ?

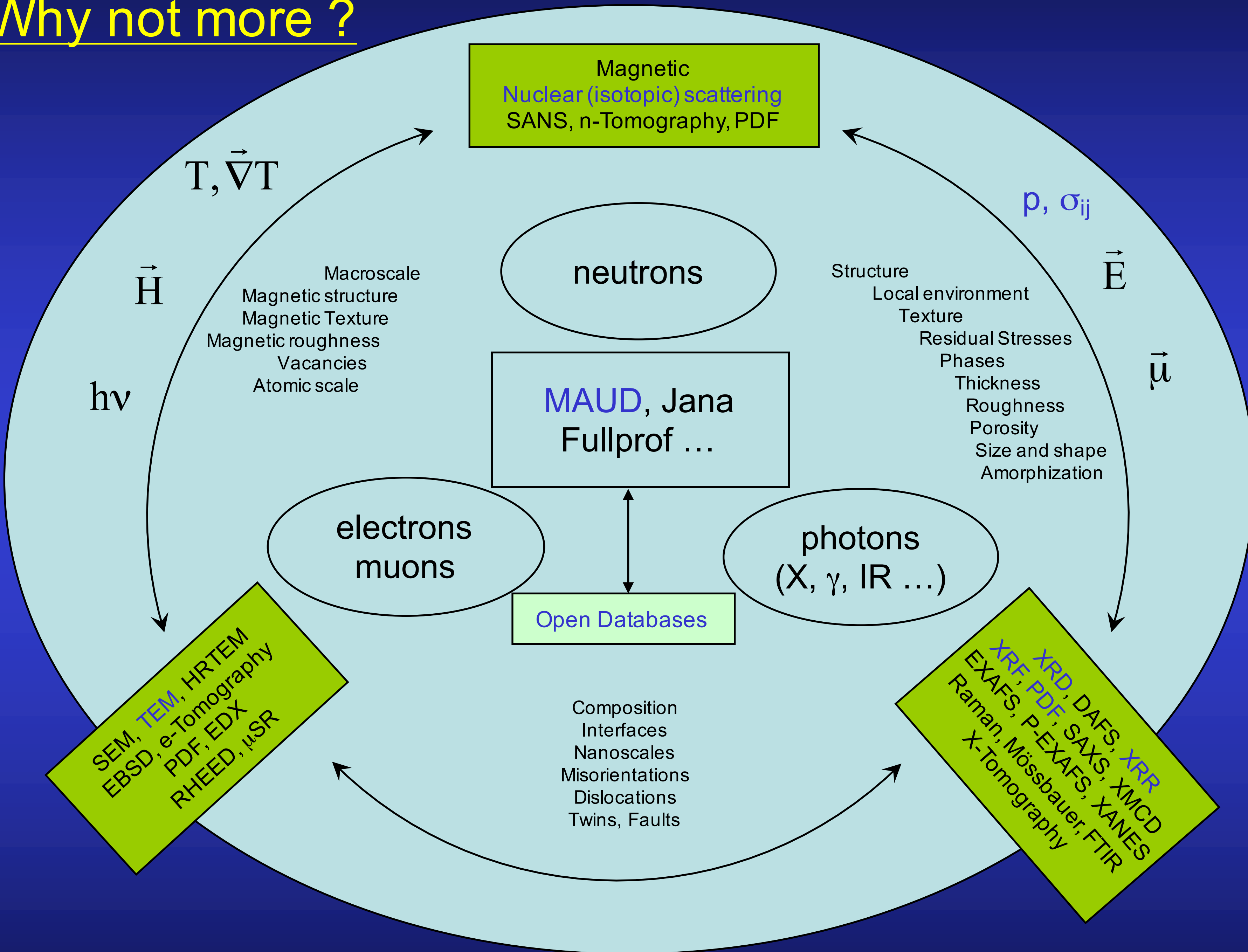
Magnetic
Nuclear (isotopic) scattering
SANS, n-Tomography, PDF
T, $\vec{\nabla}$T
$\vec{H}$
hν
p, σ_{ij}
$\vec{E}$
$\vec{\mu}$
neutrons
Macroscale
Magnetic structure
Magnetic Texture
Magnetic roughness
Vacancies
Atomic scale
Structure
Local environment
Texture
Residual Stresses
Phases
Thickness
Roughness
Porosity
Size and shape
Amorphization
MAUD, Jana
Fullprof …
electrons
muons
photons
(X, γ, IR …)
Open Databases
SEM, TEM, HRTEM
EBSD, e-Tomography
PDF, EDX
RHEED, μSR
XRD, DAFS, XRR
XRF, PDF, SAXS, XMCD
EXAFS, P-EXAFS, XANES
Raman, Mössbauer, FTIR
X-Tomography
Composition
Interfaces
Nanoscales
Misorientations
Dislocations
Twins, Faults

Conclusions

A lot of problems can be solved !

Texture helps to resolve them: good for real samples

Anisotropy favours higher resolutions

Combined analysis may be a solution, unless you can destroy your sample or are not interested in macroscopic anisotropy ...

If you think you can destroy it, perhaps think twice

Combined Analysis Workshop series:

www.ecole.ensicaen.fr/~chateign/formation/

Thanks !

UNION EUROPENNE

ESQUI
SOLSA

MEET
MIND
Xmat
COSTs

l'Europe s'engage en Basse-Normandie avec le FEDER

COMBIX: Chair of Excellence

AGENCE NATIONALE DE LA RECHERCHE ANR

FURNACE
ECOCORAIL

DAME
SEMOME

Région Centre

SMAM